J Neurophysiol 98: 3708–3730, 2007.
First published October 17, 2007; doi:10.1152/jn.00609.2007.

Neurophysiology of Prehension. III. Representation of Object Features in Posterior Parietal Cortex of the Macaque Monkey

Esther P. Gardner, K. Srinivasa Babu, Soumya Ghosh, Adam Sherwood, and Jessie Chen
Department of Physiology and Neuroscience, New York University School of Medicine, New York, New York

Submitted 29 May 2007; accepted in final form 12 October 2007

Gardner EP, Babu KS, Ghosh S, Sherwood A, Chen J. Neurophysiology of prehension. III. Representation of object features in posterior parietal cortex of the macaque monkey. *J Neurophysiol* 98: 3708–3730, 2007. First published October 17, 2007; doi:10.1152/jn.00609.2007. Neurons in posterior parietal cortex (PPC) may serve both proprioceptive and exteroceptive functions during prehension, signaling hand actions and object properties. To assess these roles, we used digital video recordings to analyze responses of 83 hand-manipulation neurons in area 5 as monkeys grasped and lifted objects that differed in shape (round and rectangular), size (large and small spheres), and location (identical rectangular blocks placed lateral and medial to the shoulder). The task contained seven stages—approach, contact, grasp, lift, hold, lower, relax—plus a pretrial interval. The four test objects evoked similar spike trains and mean rate profiles that rose significantly above baseline from approach through lift, with peak activity at contact. Although representation by the spike train of specific hand actions was stronger than distinctions between grasped objects, 34% of these neurons showed statistically significant effects of object properties or hand postures on firing rates. Somatosensory input from the hand played an important role as firing rates diverged most prominently on contact as grasp was secured. The small sphere—grasped with the most flexed hand posture—evoked the highest firing rates in 43% of the population. Twenty-one percent distinguished spheres that differed in size and weight, and 14% discriminated spheres from rectangular blocks. Location in the workspace modulated response amplitude as objects placed across the midline evoked higher firing rates than positions lateral to the shoulder. We conclude that area 5 neurons, like those in area AIP, integrate object features, hand actions, and grasp postures during prehension.

INTRODUCTION

The ability to recognize objects placed in the hand using the sense of touch is a fundamental property of the somatic sensory system. This cognitive property, called *stereognosis*, is severely impaired in humans with lesions of the parietal lobe, particularly the posterior parietal regions (reviewed in Binkofski et al. 2001; Milner and Goodale 1995; Pause and Freund 1989; Pause et al. 1989). These patients fail to shape and orient the hand properly to grasp objects and misdirect the arm during reaching. They use abnormally high levels of grip force when an object is placed in their hand and are unable to direct the fingers when asked to evaluate its size and shape.

In earlier studies of neurons in the hand representation of primary somatosensory (S-I) and posterior parietal cortex (PPC), we used digital video recordings of hand kinematics to correlate neuronal spike trains to specific actions performed by the hand as monkeys grasped and lifted objects in a trained prehension task (Debowy et al. 2001; Gardner et al. 1999, 2002, 2007a,b; Ro et al. 2000). Those studies demonstrated that activity of hand manipulation neurons in areas 5 and 7b/AIP of PPC preceded the onset of firing in S-I, peaking as the hand contacted and grasped the object. In this report, we consider how the firing rates of these neurons are influenced by properties of the grasped object. Our prehension task was designed to measure the sensitivity of cortical neurons to the intrinsic size and shape parameters of the grasped objects, and to extrinsic features such as location. Four objects were tested in each session in interleaved trials; they varied in shape (round and rectangular), size (large and small), and position in the workspace (lateral or medial to the shoulder). Two rectangles of identical size and shape placed at different positions in the workspace tested whether neural activity reflected object location or geometry. If neural activity reflected shape primitives, then firing rates should be independent of an object's location. However, if firing rates signaled location, then neighboring objects should evoke similar responses, whereas those at opposite ends of the workspace should evoke different firing rates even if they have the same shape. Furthermore, if neurons in the hand area are tuned to a specific location, as are cells in more medial regions of area 5 (Kalaska et al. 1983), their responses should become progressively weaker as objects are displaced from the preferred position.

The data presented in this report indicate that neural responses in area 5 are related to both the hand posture and intrinsic properties of the grasped object. Object selectivity is expressed as an alteration in the gain of neural responses, and their duration, rather than the presence or absence of activity during prehension.

METHODS

Neurophysiological and behavioral data were obtained from two adult rhesus monkeys (*Macaca mulatta*) trained to perform a prehension task; these animals were also used in earlier studies of PPC neurons (Gardner et al. 2007a,b). Experimental protocols were reviewed and approved by the New York University Medical Center Institutional Animal Care and Use Committee (IACUC) and are in accordance with the guiding principles for the care and use of experimental animals approved by the Councils of the American Physiological Society, the National Research Council, and the Society for Neuroscience.

Prehension task

The monkeys were trained in a grasp-and-lift task to manipulate objects placed at defined locations in the workspace. The objects were

Address for reprint requests and other correspondence: E. P. Gardner, Dept. of Physiology and Neuroscience, New York University School of Medicine, 550 First Ave., MSB 442, New York, NY 10016 (E-mail: gardne01@endeavor.med.nyu.edu).

The costs of publication of this article were defrayed in part by the payment of page charges. The article must therefore be hereby marked "*advertisement*" in accordance with 18 U.S.C. Section 1734 solely to indicate this fact.

a set of four aluminum or brass knobs mounted on a box placed 22–24 cm in front of the animal as shown in Fig. 1. We tested two round and two rectangular knobs in each session. The rectangular knobs measured 20 × 20 × 40 mm; the round knobs were 15 and 30-mm-diam spheres. Additional weights placed inside the shape box were used to compensate for the difference in object mass. The total load lifted was 108 g (small round), 137 g (rectangular block), and 242 g (large round). The knobs were typically held between the fingers and palm using a whole-hand power grasp or in a semi-precision grip between the thumb and digits 2 and 3. The animals could view the workspace and used visual guidance to position their hand on the objects.

The knob arrangement on the shape box in sessions testing the *right hand* is illustrated in Figs. 1 and 2. The knob shafts were positioned (1) slightly medial to the left shoulder, (2) at the midline, (3) aligned to the right shoulder, and (4) lateral to the right shoulder. The round knobs were placed in the center positions in the earliest sessions (Fig. 2*A*), with the two rectangular blocks at the left and right ends of the shape box (knobs 1 and 4). In the middle study period, the rectangles were placed centrally, and the round knobs at the end locations (Fig. 2*B*). Round and rectangular knobs were alternated in the late sessions (Fig. 2, *C* and *D*). During recordings from the right hemisphere, when the *left hand* was tested, the shape box was shifted to the left side of the chair. Knob 2 was aligned with the left shoulder, the round knobs were placed centrally, and the rectangles sited at the outer positions (Fig. 9).

Individual knobs were tested in blocks of 2–10 trials; the order of testing was determined by the system computer's random number generator. The location of the four knobs in the workspace was represented on the computer monitor by four identical black icons; one icon was flashed in red to indicate which knob should be lifted on that trial (Fig. 1*A*). The animal had to reach to the specified knob, grasp and lift it until an upper stop was contacted. If the correct object was lifted and held in place, the animal received a juice reward; if he chose the wrong object, he was not rewarded on that trial. Although the visual cues directed the animal's attention to a specific object on each trial, he selected the particular grasp postures used to accomplish the task goals, and the timing of the task stages. Each monkey developed its own grasp strategy that was natural, comfortable, and fluid and was used repeatedly during the period of study.

The task comprised a succession of stages characterized by a specific goal for each action, a unique pattern of underlying muscle activity expressed as kinematic behavior, and a transient mechanical event signaling goal completion and transition to the next stage. We divided the task into seven stages—approach, contact, grasp, lift, hold, lower, relax—plus an intertrial interval that preceded approach (stage 0). Stages 1–3 were required for object acquisition, stages 4 and 5 for manipulation, and stages 6 and 7 for release of the object.

We monitored hand kinematics during the task using digital video (DV) recordings of the animal's behavior synchronized to neuronal

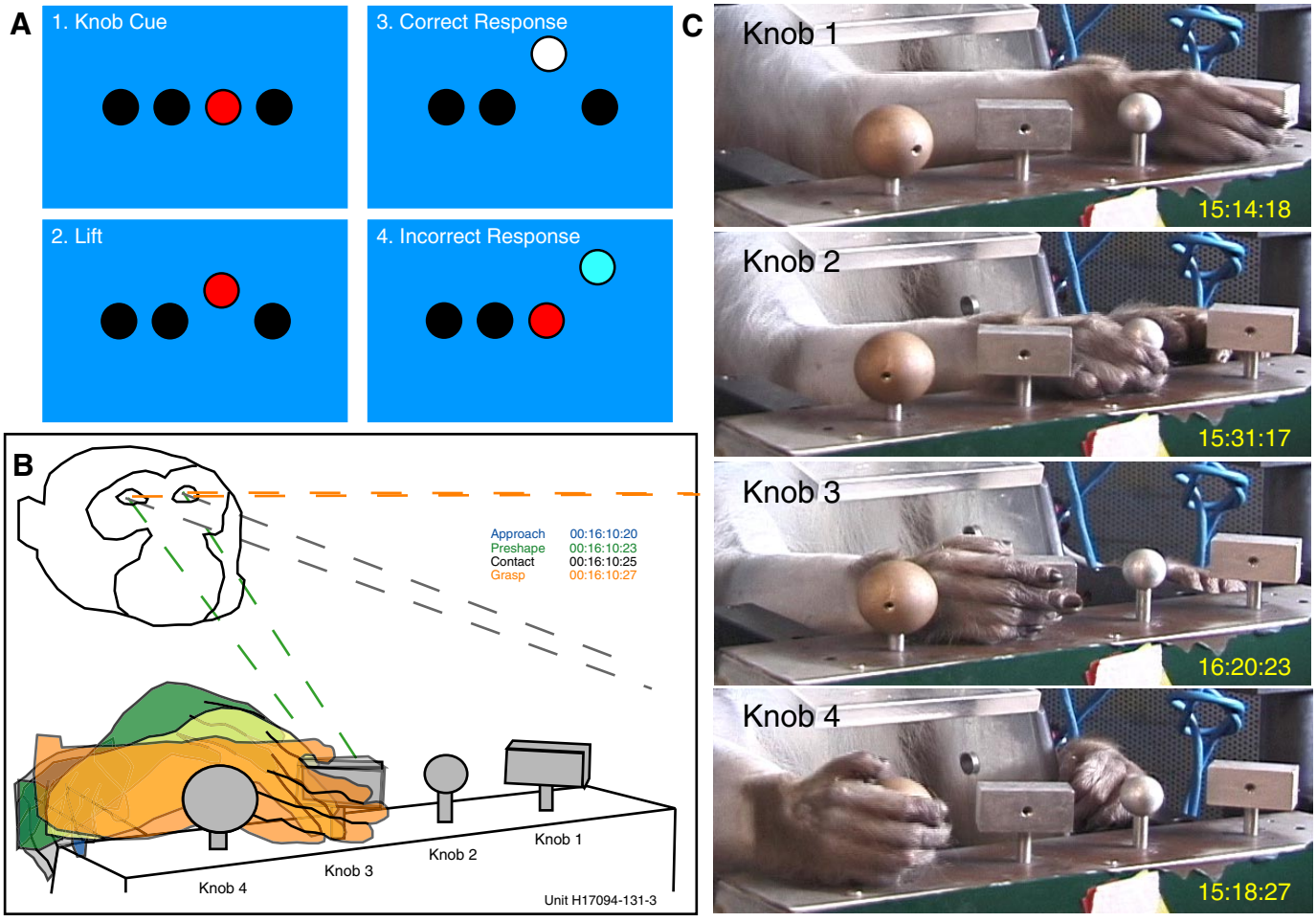

FIG. 1. Monkeys performed a trained prehension task. *A*: task cues presented to the animal on a computer monitor. The flashing red icon indicates that the animal should lift knob 3. Feedback is provided during lift by upward movement of the icon representing the knob selected on that trial; correct performance is signal by a white icon at the top position. *B*: kinematics of the approach, contact, and grasp stages traced from video images captured during task performance by *monkey H17094*. *C*: digital video images captured during task performance illustrating the hand posture used to grasp each knob. Time code specifies minute:second:frame number (30 fps) in the original DV records. Recordings from clip 1, *unit H17094-131-3*.

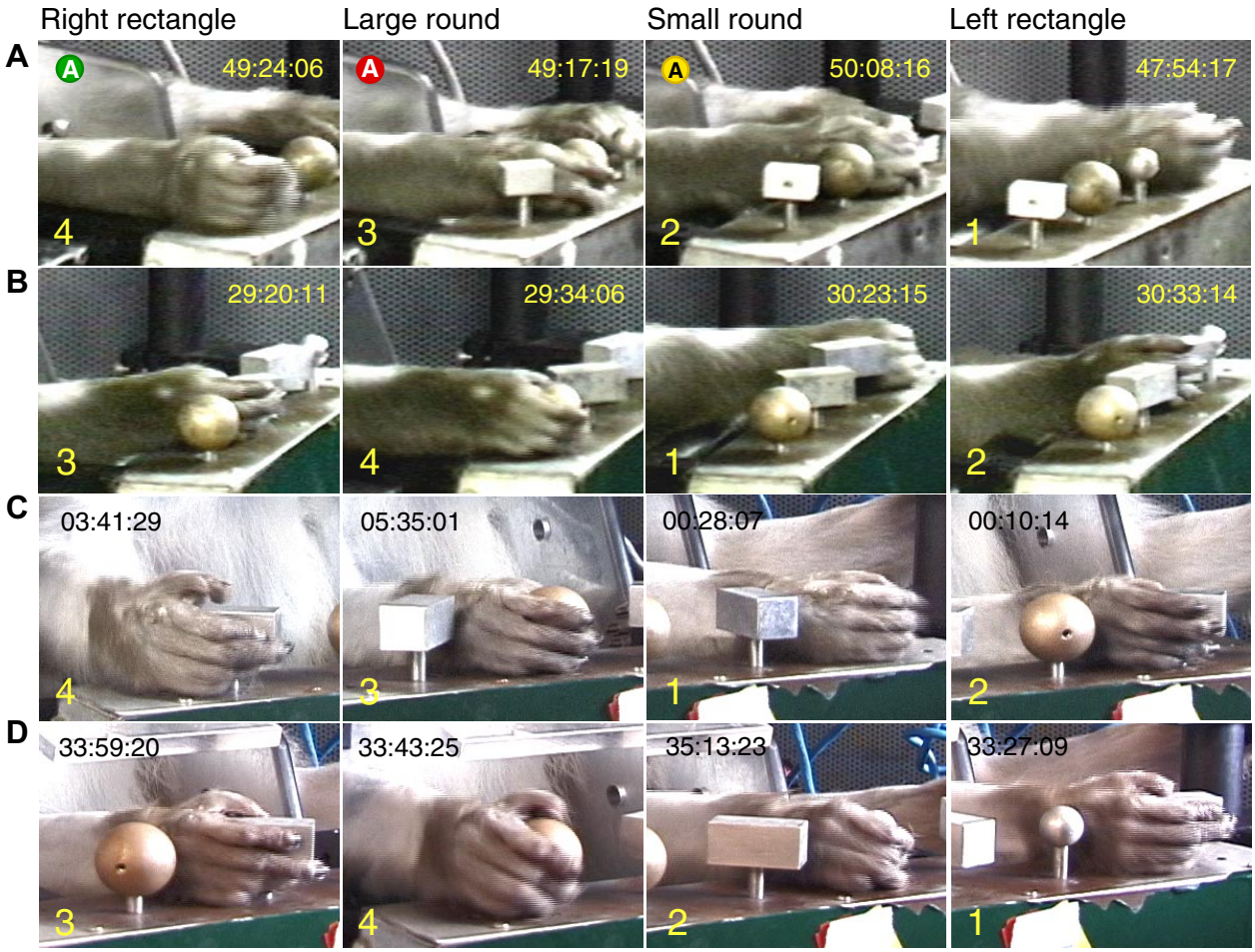

FIG. 2. Video images from sample trials illustrating the knob arrangement and grasp postures used by *monkey H17094* during the period of study. Large numbers in the *bottom left corner* of each image denote the knob position on the shape box. Note the similarity in hand postures across days and sessions. *A*: *unit H17094-10-2.4*: The rectangles were placed at the outer margins (knobs 1 and 4), and the round knobs in the center. The corresponding neural responses from are shown in Figs. 4 and 5; letters designate the matching trials in the burst analysis traces in Fig. 4. *B*: *unit H17094-70-4.2*: The round knobs were placed at the outer margins, and the rectangles in the center. *C*: *unit H17094-129-2*. *D*: *unit H17094-131-3*. Round and rectangular knobs were alternated on the shape box. Spike density plots and average firing rate graphs for the neurons in *B–D* are shown in Fig. 6, *B–D*. Images in *A* and *B* were captured in Hi8, those in *C* and *D* in DV.

spike trains, as previously described (Debowy et al. 2001, 2002; Gardner et al. 1999, 2002, 2007a,b; Ro et al. 1998). Three DV camcorders provided lateral, frontal, and overhead images of the monkey and the workspace at 29.97 frame/s. The onset of each task stage was measured from the time code of the matching video frame by visual observation, and/or by tracings of the hand posture in successive video images (Fig. 1*B*). Event time codes were stored in spreadsheets and were used subsequently as markers for display in burst analyses, alignment of neural responses in rasters and PSTHs and for bracketing task stages in statistical analyses of firing rates.

Recording and data analysis techniques

Extracellular single-unit recordings from neurons in area 5 were made in the left hemisphere of *monkeys H17094* and *N18588* and in the right hemisphere of *N18588* as described in Gardner et al. (2007a); the specific recording locations are illustrated in Fig. 3. Spike trains were digitized at 16-bit resolution, 48 kHz, or 12-bit resolution, 32 kHz by the DV camcorders and stored as an audio trace together with video records of the hand actions. Video clips of the animal's behavior and the digitized spike trains were downloaded to the lab computers and stored as both QuickTime files, and in Audio Interchange file format (AIFF) for quantitative analyses of firing patterns. As video and spike trains were recorded and digitized simultaneously, both datasets spanned the same time interval. Hence knowledge of the time code of each video frame in the clip provided a precise way to locate the matching firing patterns. Similarly, measurements of the timing of spikes with respect to the onset of the audio data sample placed each spike in a precisely designated video frame.

The spike trains of each neuron were analyzed using custom designed software (Sherwood et al. 2006) written in Igor Pro 5 (WaveMetrics). Neural responses during the task were screened initially with *burst analysis* graphs (Fig. 4) that provide a continuous record of neural and behavioral events within each video clip. This technique automatically detects periods of high neural activity in which the firing rate exceeds one SD above the mean rate per 100-ms bin (white "burst threshold" trace); pulses on the green "burst" trace mark the mean firing rate and duration of these epochs. Reverse correlation of the burst onset, peak, and end times with the matching video images of the monkey's behavior highlighted the behaviors to which the neuron was most responsive.

The single trial responses depicted in burst analysis traces were complemented by more standard multi-trial analyses. Spike *rasters* and peristimulus time histograms (PSTHs), aligned to the video frame

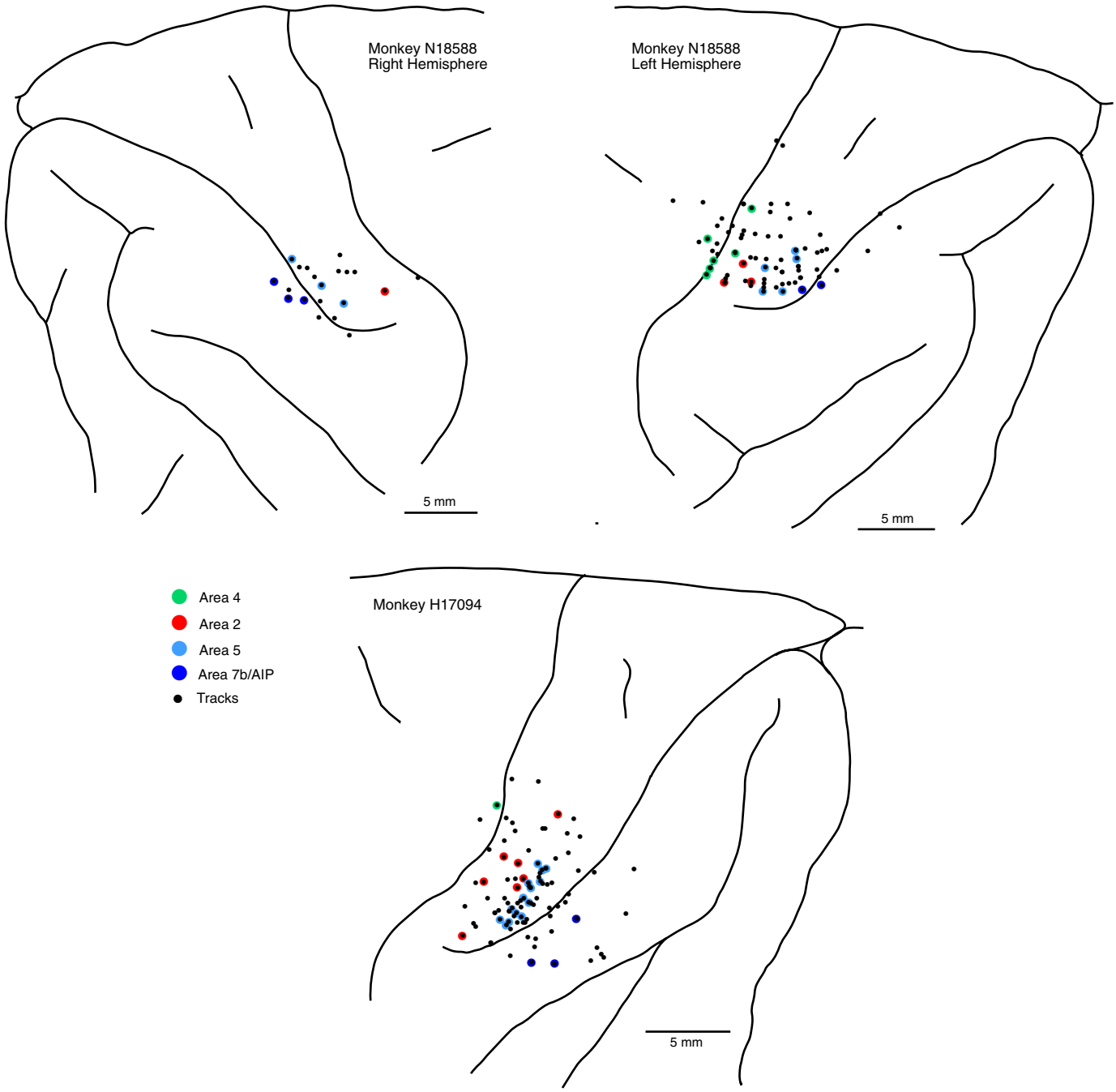

FIG. 3. Cortical recording sites in *monkeys N18588* and *H17094*. Colored markers denote sites where task-related neurons were recorded; dots, electrode entry points of other tracks. Recordings in the right hemisphere of *N18588* were performed using 3- or 4-electrode arrays centered at the marked sites.

onset times of hand contact with the knob, were used to measure the consistency and reliability of neural responses (Fig. 5). PSTHs were smoothed to create spike density functions of firing rate as a function of time using a 50-ms window displaced every 10 ms (de Lafuente and Romo 2006).

The task-evoked spike trains were subdivided into stages linked to the actions viewed in the video records, allowing us to calculate *mean firing rates per stage* for each trial. Trials were grouped by knob and reach style to compute average firing rate profiles for each knob (Fig. 6), and for statistical analyses. A repeated-measures ANOVA model (StatView, SAS Institute) analyzed whether there was significant modulation of firing rates across the seven task stages and the pretrial interval for each trial (F-test, $P < 0.05$), and whether the knob identity (size, shape and/or location) was a significant between subjects factor.

We also evaluated neural tuning to specific objects using a variety of selectivity indices. Object selectivity among the four test knobs was evaluated during each task stage using the preference index (PI)

$$\mathrm{PI} = 100 * [(n - (K_1 + K_2 + \cdots + K_n)/K_{max})/(n - 1)] \quad (1)$$

where n = the number of objects tested, K_i = the response to object i, and K_{max} = the strongest response during a particular action. The PI has been used to measure object selectivity of neurons in area AIP and in frontal motor areas (Murata et al. 2000; Raos et al. 2004, 2006; Umilta et al. 2007) and to evaluate hand muscle synergies in monkeys during similar tasks (Brochier et al. 2004).

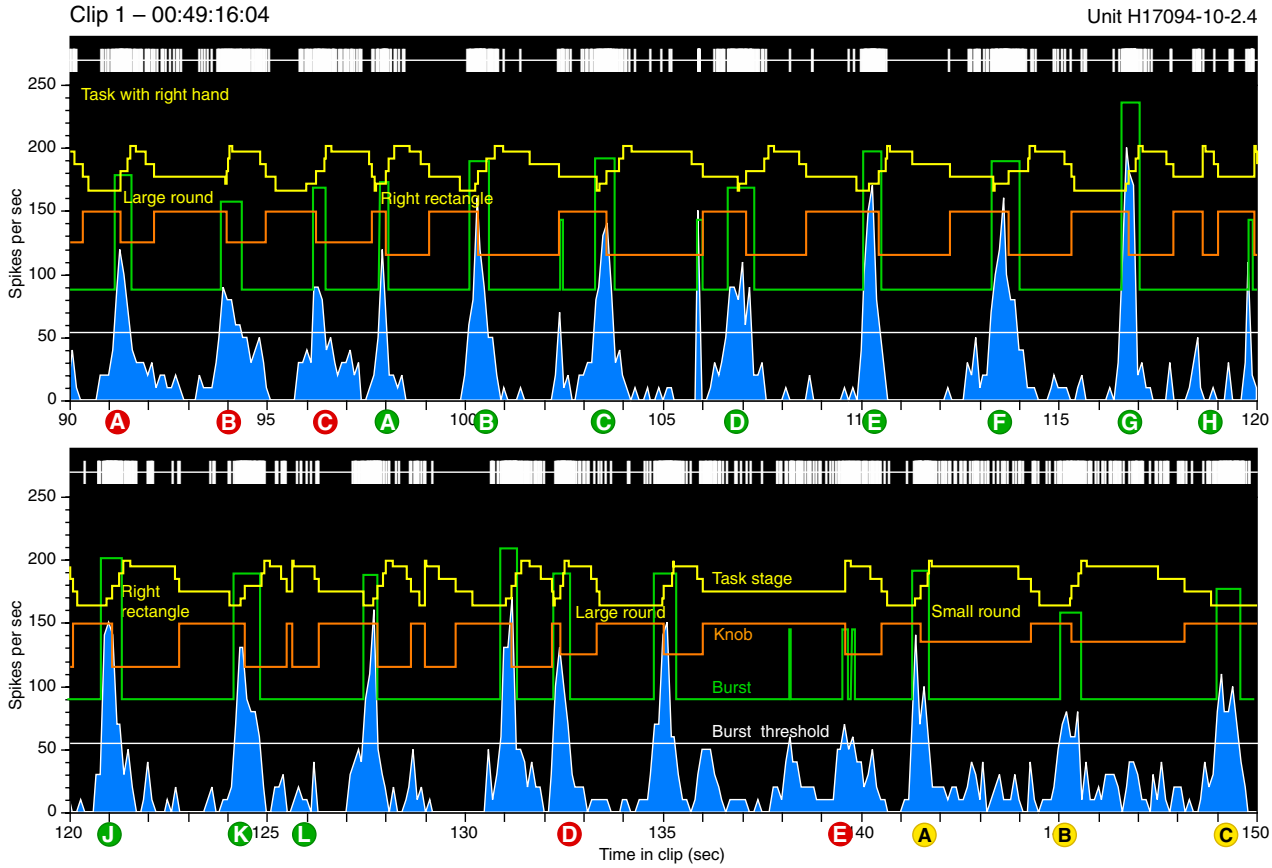

FIG. 4. Burst analysis graphs of continuous neural and behavioral activity recorded from *unit H17094-10-2.4* during a 60-s period. The spike train was binned in 100-ms intervals (blue graph) to compute continuous firing rates. Yellow task stage trace: each stepped yellow pyramid marks a single trial. Upward deflections denote the start of stages 1–4 (approach through lift); downward deflections mark the onset of stages 5–8 (hold through release). Neural responses began at approach and peaked at contact. The animal did not relax the grasp on some trials of the right rectangle (green H, L) and the large sphere (red E) but simply lifted the knob again; neural responses were much weaker on these incomplete trials. Orange knob trace: downward pulses that span the contact through lower stages indicate the knob location on the shape box and the duration of hand contact. The pulse amplitude is proportional to the knob distance from the left edge of the box. White burst threshold trace: firing rate set 1 SD above the mean rate during the entire 2.5-min video clip. Green burst trace: upward pulses mark periods when continuous firing rates exceeded the burst threshold; the burst pulse amplitude indicates the mean firing rate during this interval. The burst trace has been displaced by 90 spike/s to improve readability. Images keyed to the grasp stage of specific trials are shown in Fig. 2.

As in these other neural studies, we also computed the differential PI (dPI) for each task stage

$$\text{dPI} = 100 * (\text{max} - \text{min})/(\text{max} + \text{min}) \quad (2)$$

where max and min are the maximum and minimum responses per stage regardless of which object evoked that activity.

The effects of object size, shape, and location on neural responses were assessed using similar indices. The size index compared responses to the two round knobs

$$\text{Size Index} = 100 * (\text{small} - \text{large})/(\text{small} + \text{large}) \quad (3)$$

The place index compared responses to the two rectangular knobs

$$\text{Place Index} = 100 * (\text{right} - \text{left})/(\text{right} + \text{left}) \quad (4)$$

Positive values indicate preferences for the small round and right rectangular knobs; negative values denote preferences for the large round and left rectangular knobs.

To test the role of object shape primitives, we pooled trials of the large and small spheres (round) and the left and right rectangular blocks (rectangle)

$$\text{Shape Index} = 100 * (\text{round} - \text{rectangle})/(\text{round} + \text{rectangle}) \quad (5)$$

RESULTS

This report describes the prehension responses of 83 neurons recorded in the hand representation of area 5 in the posterior parietal cortex of two monkeys (left hemisphere, $n = 52$; right hemisphere, $n = 31$). These cells were tested systematically with four objects and comprise a subset of the population described in our earlier studies of PPC (Gardner et al. 2007a). All of the neurons were studied over a minimum of 50 trials and showed highly significant modulation of firing rates across the task stages ($P \leq 0.0001$). The mean number of trials per neuron in *monkey H17094* was 123.6 ± 7.8, evenly distributed among the four knobs (mean = 30.9 ± 1.1 trial/knob). The mean number of trials per neuron in *monkey N18588* was 89.6 ± 4.4; mean total trial/knob ranged from 16.6 ± 1.5 for the small sphere to 25.9 ± 0.8 for the large sphere with an average per knob of 22.4 ± 0.7 trials. We also analyzed responses of 32 neurons in adjacent regions of S-I cortex and area AIP/7b in these animals (Table 1).

Both animals performed the task using a continuous sequence of hand movements from approach through lift. Object acquisition and manipulatory actions were similar in time course to the coordination of grip and load forces reported in

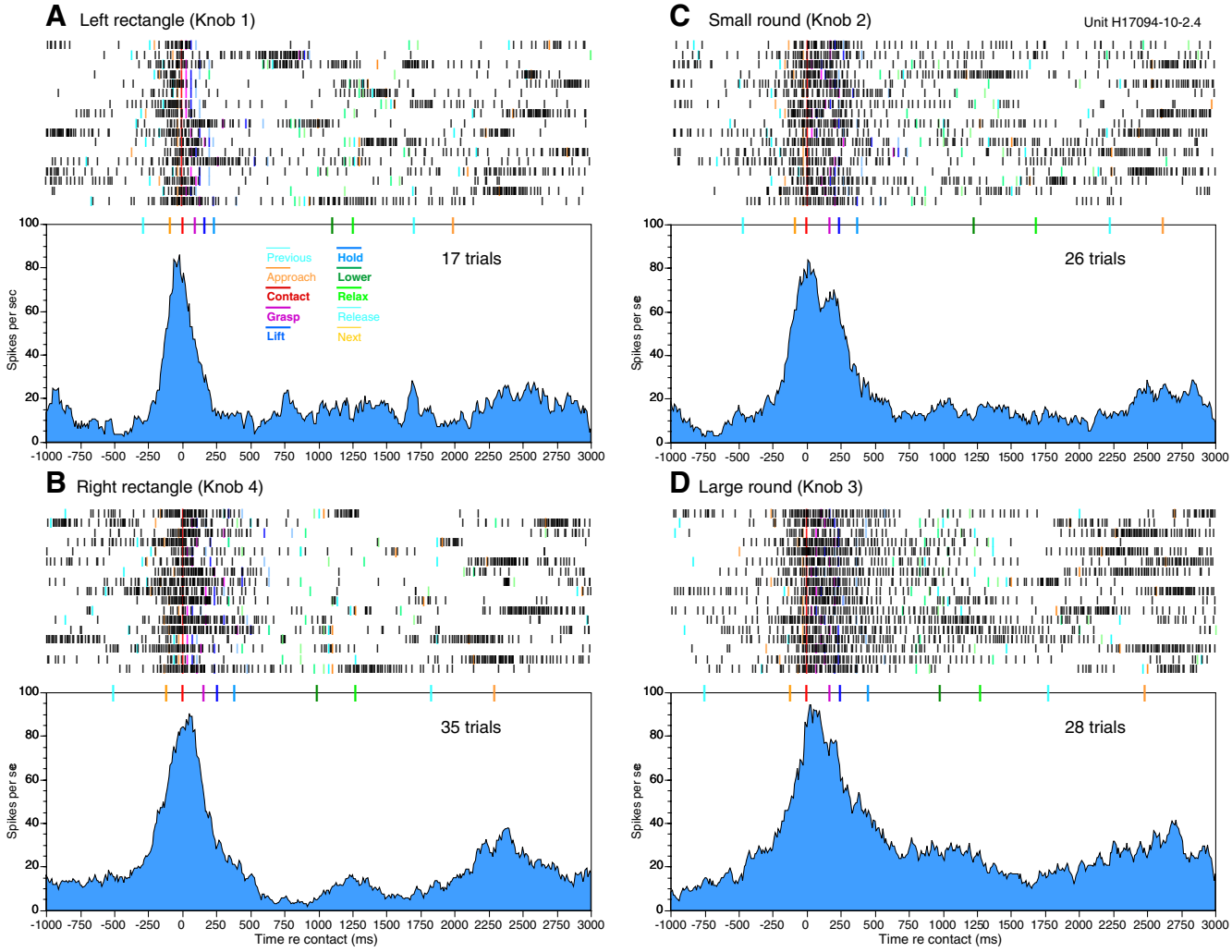

FIG. 5. Rasters of the 1st 17 trials of each knob aligned to hand contact and spike density functions averaging all knob trials for the neuron shown in Figs. 2 and 4. Colored markers on the raster show the onset times of the task stages; markers above the spike density graphs show the mean onset times of the stages averaged across the trials. Although all 4 knobs evoked the same peak firing rates at contact, the spike trains were of longer duration for the round knobs, persisting through the hold stage. Spike bursts near the right margin represent responses on the next trial (gold marker).

studies of precision grip in humans (Johansson 1996; Johansson and Cole 1992; Westling and Johansson 1984, 1987). The animals differed in the hand tested and the grasp postures used to acquire objects.

Area 5 neurons respond most vigorously to acquisition of diverse objects

Monkey H17094 was trained to perform the task with the right hand as recordings were made in the left hemisphere. He approached the knobs from above, targeting the right side of each knob (Fig. 1*B*). The objects were grasped with the palm placed to the right, and the fingers aligned parallel to the frontal plane (Fig. 1*C*). Although the left and right rectangles were often positioned at opposite ends of the shape box, they were grasped with the same hand posture with the digits extended. The round knobs were grasped with greater flexion of the digits with the ulnar fingers placed below the knob. The small round knob was usually clasped at its base in a semi-precision grip between the thumb and digits 2 and 3 and rarely contacted the palm; the large sphere contacted all 5 digits and the palm pads (Fig. 2). Both spheres were scooped up during lift with the load force concentrated on the digit shafts; the tight grip and flexed hand posture was maintained through the hold stage. The hand postures used in the initial tracks (Fig. 2*A*) were preserved almost unchanged throughout the period of study regardless of the actual location of the knobs on the shape box.

Figure 4 illustrates continuous spike trains and markers of the task stages recorded over a 60-s period during the session shown in Fig. 2*A*. Each of the stepped pyramids in the yellow task stage trace denotes a trial of the prehension task. The neural responses began at or before the onset of approach (initial step in the task stage trace). The firing rate increased abruptly as the animal projected the arm toward the target object with peak activity at contact, and then subsided during lift (highest pulse in the task trace). The spike trains decayed to low levels during holding, and returned to or below baseline in the late task stages as grasp was relaxed. Spontaneous activity between trials was weak or absent.

Although the temporal pattern of the neural response was similar on each trial, the peak firing rate and response duration differed depending on the object tested (orange knob trace), the

speed of acquisition, and the previous history of stimulation. The longest duration spike trains in these records occurred when the large round knob was tested (red A–C). Responses to successive trials of the same object decreased in peak rate regardless of shape, particularly if the animal lifted the object without prior relaxation of the grip (red E, green F, J).

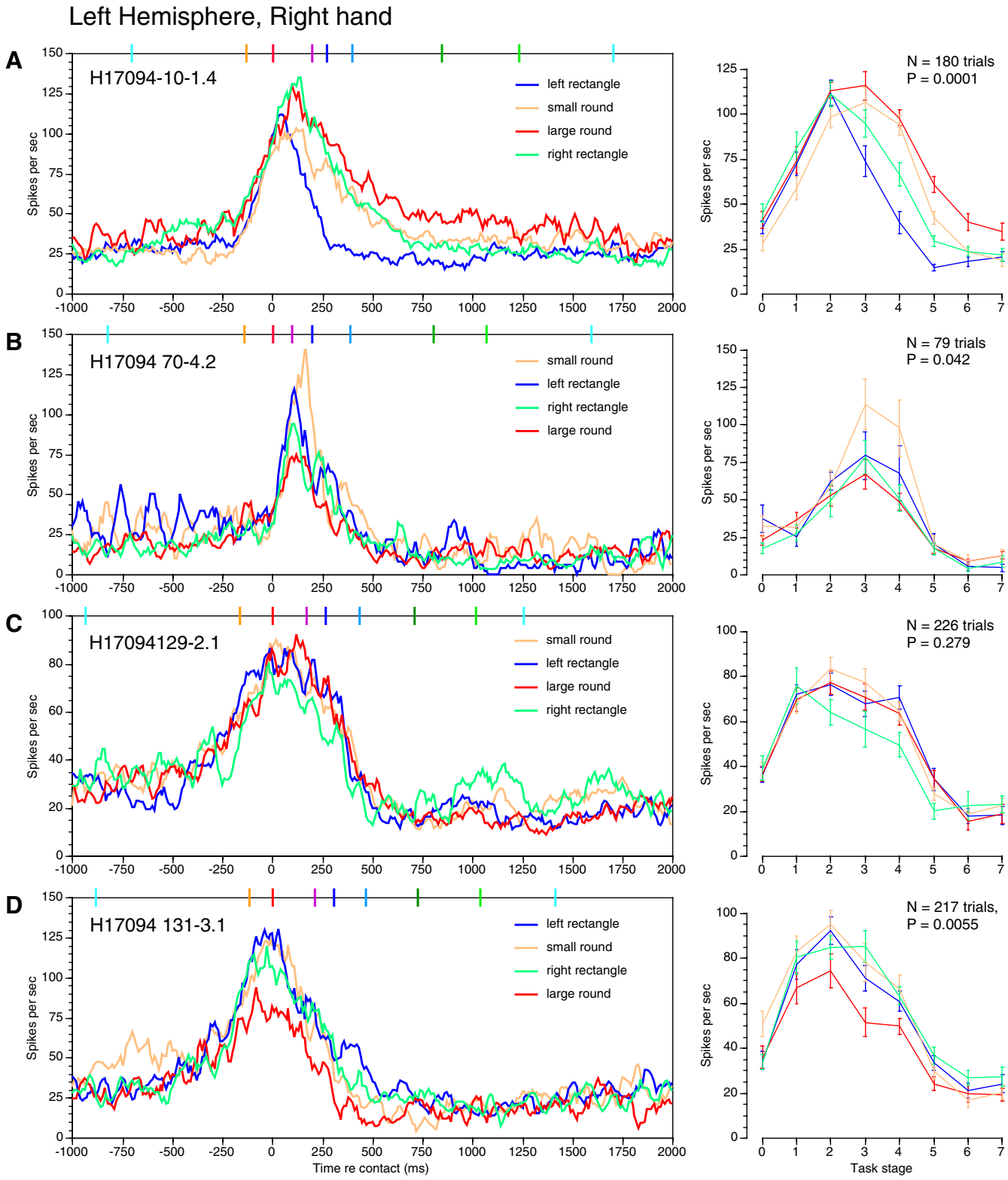

FIG. 6. Superimposed spike density functions (*left*) and average firing rates (±SE) per task stage (*right*) for 4 neurons illustrating the range of selectivity for specific objects observed in *monkey H17094.* Stage 0 indicates the pretrial interval. Knob preferences are generally highest in stages 2–4; in these examples, the round knobs evoked the highest firing rates. *P* values in the *right panels* indicate the selectivity for knobs as determined by repeated-measures ANOVA analyses. The order of listing of the knobs in the keys denotes their left-to-right locations on the shape box. Images of the hand postures used to grasp each of the knobs are shown in Fig. 2.

TABLE 1. *Object selectivity in parietal cortex*

	H17094		N18588		Both Animals	
	Total Cells	Percent Total	Total Cells	Percent Total	Total Cells	Percent Total
Area 5						
Total cells analyzed (L)	46		6		83	
Total cells analyzed (R)	0		31			
Significant knob	19	41.3	9	24.3	28	33.7
Significant knob*rate	14	30.4	16	43.2	30	36.1
Significant size	15	32.6	2	5.4	17	20.5
Significant place	5	10.9	8	21.6	13	15.7
Significant shape	11	23.9	1	2.7	12	14.5
Area 7b/AIP						
Total cells analyzed (L)			6		14	
Total cells analyzed (R)			8			
Significant knob			5	35.7	5	35.7
Significant knob*rate			4	28.6	4	28.6
Significant size			4	28.6	4	28.6
Significant place			3	21.4	3	21.4
Significant shape			2	14.3	2	14.3
S-I Cortex						
Total cells analyzed (L)	10		8		18	
Total cells analyzed (R)						
Significant knob	4	40.0	7	87.5	11	61.1
Significant knob*rate	4	40.0	4	50.0	8	44.4
Significant size	0	0.0	3	37.5	3	16.7
Significant place	6	60.0	4	50.0	10	55.6
Significant shape	0	0.0	6	75.0	6	33.3

Rasters and spike density plots aligned to hand contact with the knob provide an expanded view of the spike trains evoked by each of the four knobs (Fig. 5). Firing patterns during the initial acquisition stages were nearly identical for these objects, yielding similar maximum rates at contact (red markers). However, the responses diverged as grasp was secured (magenta marker) and the knob lifted (dark blue marker). The two rectangular knobs (Fig. 5, *A* and *B*) produced shorter spike bursts than the round ones as the firing rates dropped precipitously during lift and returned to baseline or below during the hold stage (light blue). Although the two rectangles were positioned at opposite ends of the shape box, they evoked very similar neural responses apparently because they were grasped with nearly identical hand postures.

In contrast, responses to the large round knob persisted throughout the trial, remaining substantially higher than baseline during the lift and hold stages (Fig. 5*D*); firing rates did not subside until the object was lowered and the grasp relaxed (green markers). The large sphere was the heaviest knob, requiring the greatest grip and load forces to maintain lift during the hold stage. As a result, the mean duration of the hold stage was briefest for this object in both animals (Table 2). Responses to the small round knob were intermediate between the rectangles and the large round knob (Fig. 5*C*).

The range of object selectivity observed in this animal is illustrated in Fig. 6 by superimposed, smoothed spike density plots and average firing rate graphs from four different cortical neurons; the corresponding grasp postures are provided in Fig.

TABLE 2. *Mean task stage duration (ms)*

	Small Round	Large Round	Medial Rectangle	Lateral Rectangle
H17094 (46)				
0 Pretrial	652.9 ± 15.6	687.0 ± 15.1	604.4 ± 26.0	648.9 ± 19.9
1 Approach	157.3 ± 8.4	126.5 ± 5.1	125.6 ± 5.5	123.8 ± 5.9
2 Contact	169.5 ± 9.3	139.6 ± 9.5	128.9 ± 6.4	157.2 ± 9.2
3 Grasp	81.1 ± 3.7	94.5 ± 5.2	101.4 ± 11.0	114.3 ± 9.0
4 Lift	152.8 ± 4.8	188.9 ± 5.3	131.7 ± 6.8	169.1 ± 3.7
5 Hold	476.9 ± 25.1	345.8 ± 14.8	447.4 ± 31.6	353.0 ± 18.5
6 Lower	380.5 ± 23.3	318.1 ± 14.6	256.6 ± 15.6	281.0 ± 14.8
7 Relax	480.2 ± 38.3	461.6 ± 35.0	552.5 ± 34.4	578.1 ± 40.3
N18588 (37)				
0 Pretrial	742.2 ± 13.6	753.5 ± 8.7	703.0 ± 11.0	740.7 ± 11.3
1 Approach	208.6 ± 13.2	199.8 ± 6.1	257.6 ± 12.4	207.1 ± 6.6
2 Contact	214.2 ± 15.3	154.0 ± 17.3	170.3 ± 22.7	135.1 ± 22.7
3 Grasp	83.3 ± 5.5	41.3 ± 2.7	42.8 ± 4.1	41.7 ± 3.6
4 Lift	122.3 ± 9.7	97.7 ± 6.7	84.5 ± 6.3	125.1 ± 5.5
5 Hold	503.4 ± 26.9	203.8 ± 6.5	547.3 ± 34.3	324.7 ± 19.3
6 Lower	214.7 ± 13.9	279.0 ± 17.8	244.2 ± 11.7	310.1 ± 18.7
7 Relax	545.7 ± 26.8	769.4 ± 45.7	438.0 ± 36.9	634.1 ± 28.1

Values are means ± SE. Number of cells is in parentheses.

2. All of the neurons analyzed responded to the four test objects, but the amplitude and/or duration of the spike train varied between neurons and objects. Distinctions in firing rates between objects, when present, usually occurred after contact as the hand was moved over the object surface and during grasp and lift actions.

The neuron in Fig. 6*A* was one of the most highly selective for shape in the population analyzed. It was recorded on the same track as the neuron in Figs. 4 and 5; it shared a similar strong preference for the large round knob after contact and responded least to the left rectangle. Although the firing rates evoked by each object were nearly indistinguishable during approach, they diverged after contact. The greatest spread in firing rates occurred during lift, when view of the knob was partially obscured by the animal's hand. The differences in mean firing rates between knobs across the seven task stages were highly significant [$F(3,176) = 11.9$, $P < 0.0001$], as were interactions between firing rate per stage and knobs [$F(7,21) = 4.81$, $P < 0.0001$].

The spike trains of the neuron in Fig. 6*B* were modulated by the size, shape, and location of the knobs during the grasp and lift stages but not during other task actions. It responded most vigorously to the small round knob during the preferred stages and least to the large round knob. The difference in mean firing rates was significant [$F(3,73) = 2.87$, $P = 0.042$]. The small sphere was the lightest object and was grasped with the most flexed hand posture (Fig. 2*B*). It was placed at the most medial location on the shape box (knob 1) and was furthest from the test hand; the large sphere was located at the most lateral position (knob 4). Responses to the two rectangular knobs during grasping were intermediate between the round knobs, reflecting their central locations on the shape box.

The neurons in Fig. 6, *C* and *D,* were typical of the majority of cells, showing only subtle distinctions in firing patterns between knobs. Representation by the spike train of hand actions during the task was stronger than the distinctions between grasped objects. Responses to three of the four knobs overlapped and did not differ significantly ($P > 0.05$). The remaining knob evoked weaker responses than the other three; in these examples, knob 4 placed lateral to the animal's hand produced the lowest firing rates (Fig. 2, *C* and *D*). The spread in firing rates was clearest during stages 3 and 4 and were minimal during approach before the objects were touched.

Weak object selectivity was observed in both animals, and was independent of the laterality of the recording site in the brain. Figure 7 shows a 33-s epoch of recordings made simultaneously on three electrodes placed in the right hemisphere of *monkey N18588,* which was trained to use its left hand. Like the continuous responses shown in Fig. 4, the four neurons illustrated began their responses at the onset of approach and fired maximally at contact and during grasping of each knob. Their firing rates returned to baseline at the start of lift. Synchronized responses occurred across all of the recording sites during the initial task stages but not in later stages nor during other movements such as licking the juice tube on reward delivery (magenta trace). The neurons distinguished whether acquisition was completed (A, C, E, G, and J) or if the trial was aborted after contact (B). Similarly, lift of a knob without prior relaxation of grasp (F, H) evoked weaker responses than trials in which all of the task actions were performed (E, G).

Superimposed spike density functions and average firing rate graphs are shown in Fig. 8, *A* and *B,* for two of these neurons, together with similar records from another pair of cells from a different recording session (Fig. 8, *C* and *D*). Like the neurons from the left hemisphere illustrated in Fig. 6, the spike density plots evoked by all four objects were similar in time course with peak activity at contact or during grasping, and a precipitous drop in firing during lift. The most striking feature of the data are the overlap in spike trains evoked by the four knobs, particularly during approach. Only one of these neurons showed significant differences in firing rates (Fig. 8*D,* $P < 0.05$); it responded best to the large sphere and least to the small one. The weakest responses in three of the cells occurred on trials testing the left rectangle that was placed at the most lateral position in the workspace; the fourth neuron responded least to the small round knob. The varying neuronal responses are particularly striking because they were obtained during the exact same trials on different electrodes.

The average firing rates per stage diverged more sharply than the PSTHs apparently because of differences in stage duration between objects (Table 2). The small round knob evoked high firing rates in stages 1 and 2; firing rates during static grasp and lift were generally lower than for the other objects. The small sphere required the longest acquisition times; the mean duration of stages 2–4 was 120 ms longer for this knob than for the other three objects. The large round knob evoked the highest firing rates during lift and hold actions but was retained in the hold posture for the shortest interval. The hold stage for the large sphere was 120 ms shorter than that of the neighboring left rectangle and >300 ms less than the hold stage of the small sphere and the medial rectangle.

Images of the grasp posture used by this animal suggest that the timing differences may have resulted from the hand kinematics used to grasp these objects (Fig. 9). This monkey did not fully enclose the large knobs in his hand. Instead he placed his fingers below the two rectangles and the large sphere and scooped them up with the wrist supinated. In contrast, the small sphere was usually clasped in a semi-precision grip between the thumb and digits 2 and 3 with hand postures similar to those used by *monkey H17094.* The formation of the precision grip resulted in longer duration contact, grasp, and hold stages for the small round knob (Table 2).

We also recorded responses to prehension in the left hemisphere of this animal with similar results (Fig. 10, *A* and *B*). Only one of six neurons analyzed in area 5 of the left hemisphere showed significant knob preferences; the small round knob was the preferred object. Neurons in adjacent regions of S-I and area AIP/7b showed greater object selectivity than those in area 5; examples are provided in Fig. 10, *C* and *F,* for completeness. However, the small number of neurons sampled precludes definitive conclusions concerning the prevalence of object selectivity in these regions (see Table 1).

Population distribution of object selectivity in area 5

The trends observed in the data from individual neurons in area 5 were clearly evident when responses of all cells studied were quantified statistically. Mean firing rates per stage were computed for each neuron on a trial-by-trial basis, and analyzed using repeated-measures ANOVA protocols with knob type as a between subjects factor. One-third of the neurons

FIG. 7. Burst analysis records from 4 simultaneously recorded neurons in *monkey 18588.* Same format for burst traces as in Fig. 5; the colored spike rasters at the top correspond to the matching colored histograms in the burst traces. The neurons show coincident firing during object acquisition but not during other actions. The magenta *tongue* trace shows actions of the tongue as the animal licked the juice tube for reward. The 1st upward deflection indicates mouth opening and tongue protrusion, the 2nd upward deflection indicates full extension of the tongue; downward deflection marks retraction of the tongue into the mouth. Only the neuron in *D* responded to tongue movements. *A* and *B*: *units 313_1–2.1* (*A*) and *313_1-2.4* (*B*) recorded on electrode 1. *C*: *unit 313_2-2.2* recorded on electrode 2. *D*: *unit 313_4-2.3* recorded on electrode 4. Images of the hand actions in these records are provided in Fig. 9, *A* and *B*.

tested (28/83) showed statistically significant differences in firing rates ($P < 0.05$) as a function of knob tested during the seven task stages (Table 1). Thirty-six percent of neurons showed significant interactions between firing rate per stage and knob, indicating preferences for particular objects during some actions but not during others. Object selectivity was higher in *monkey H17094* than in *N18588.*

Despite differences in grasp style, the neurons recorded in both animals showed similar preferences for particular actions, objects, and places within the workspace during task performance (Fig. 11). Peak responses in the population occurred most frequently at contact and during grasp (stages 2 and 3) when the hand first engaged directly with the knobs (Fig. 11*C*). The small round knob was the most preferred object in both animals, evoking maximum responses in 43% of the population (Fig. 11*A*: *H17094* = 20/46 neurons; *N18588* = 13/31 neurons). This knob was placed at the midline in 13/13 cells in the right hemisphere of *monkey N18588,* in 8/20 cells in *monkey H17094,* and at the most medial location in the remaining 12 cells in *H17094*. Of the 28 neurons that showed statistically significant effects of object on firing rates, 13 (46%) preferred the small sphere, 6 (21%) preferred the large sphere, 6 preferred the medial rectangle, and 3 favored the lateral rectangle.

The medial rectangle was the next most preferred object in both animals. The left rectangle was more likely to evoke peak activity when tested with the right hand, and the right rectangle was favored in trials testing the left hand (Fig. 11*A*). The object placed

at the most lateral position was the least likely to evoke maximum firing (Fig. 11*B*: knob 4 in *H17094* and knob 1 in *N18588*). As a result, the large round knob and the lateral rectangle were the least preferred objects in terms of peak firing rates, in part because they were located in front of or lateral to the test arm, and were easiest to regrasp on subsequent trials.

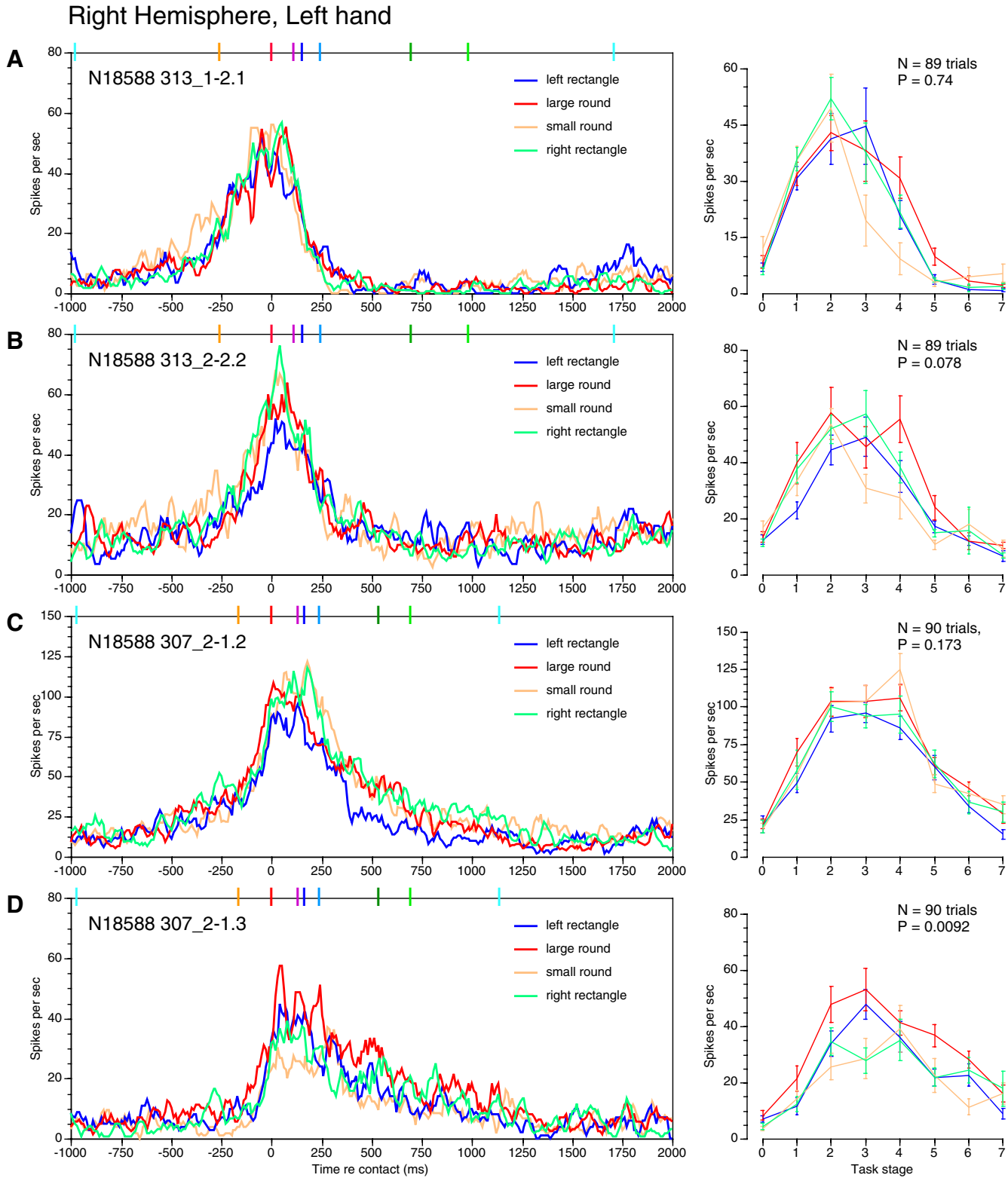

FIG. 8. Superimposed spike density functions (*left*) and average firing rate graphs (*right*) illustrating the range of object selectivity observed in *monkey N18588;* same format as Fig. 6. *A* and *B*: simultaneously recorded neurons from 2 different electrodes on track 313; burst analysis records for these cells are shown in Fig. 7, *A* and *C*. *C* and *D*: neurons recorded simultaneously by the same electrode on track 307. Images captured from the digital video recordings for these cells are shown in Fig. 9, *C* and *D*. Only the neuron in *D* showed a significant knob preference, responding best to the large sphere.

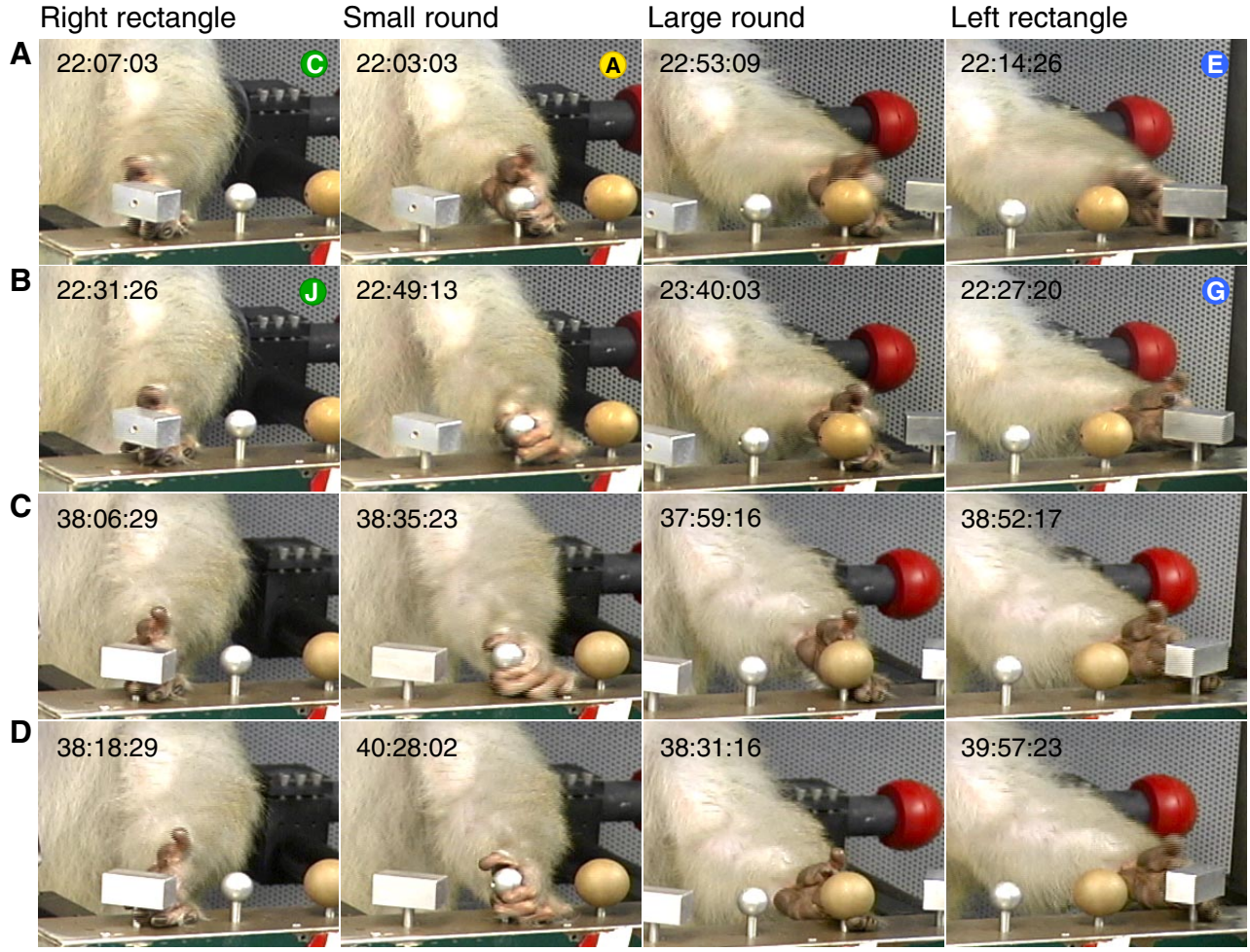

FIG. 9. Digital video images of the grasp postures used for the 4 knobs by *monkey N18588.* Spike density plots and average firing rate graphs for these neurons are shown in Fig. 8. *A* and *B*: image captures from clip 7 of track 313. Letters designate the corresponding trials in the burst analysis records in Fig. 7. *C* and *D*: image captures from clip 5 of track 307. Note the similarity in hand postures across days and sessions. Only the small round knob is fully grasped in the hand; the others are held with the digits extended.

Selectivity among the four objects during each stage was also assessed using the PI and dPI as described in METHODS. These metrics do not make assumptions about the specific characteristics of objects that yield maximum and minimum responses; they have been used in other studies to assess object selectivity of neurons recorded in areas AIP, F5, F2vr, and M1 during similar prehension tasks (Murata et al. 2000; Raos et al. 2004, 2006; Umilta et al. 2007). Figure 12 plots PI and dPI values for the neurons illustrated in Figs. 6 and 8; both indices yielded nearly identical results. Although the firing rates of these neurons were highest in stages 1–3, the index values were lowest during these acquisition stages. The highest values of PI and dPI were recorded in stages 4 and 5 (lift and hold) when firing rates dropped back to baseline. PI and dPI values sometimes exceeded 50 in stage 5 when neurons fired at low rates to the most preferred knob, and were nearly silent for the least effective one (Fig. 12, *A* and *E*). These findings suggest that metrics such as the PI and dPI exaggerate differences in firing rates when neural responses are weak and minimize them when neurons are most responsive.

We used similar techniques to measure the relative influence of object size, shape, and location on mean firing rates per stage. To analyze the effect of object size, we compared responses to the small and large spheres. Twenty-one percent of area 5 neurons (17/83) showed significant effects of object size on task responses in repeated-measures ANOVA analyses (Table 1); size selectivity was higher in *monkey H17094.*

The size index allowed us to compare which knob was preferred during specific task stages. The small round knob was generally favored during object acquisition but rarely during lift and hold actions (black curves, Fig. 13). The large round knob was the most preferred object in stage 5 in both animals (*H17094* = 16/49 cells; *N18588* = 23/31 cells), and the small round knob was the least preferred in the hold stage.

The knob location in the workspace had weaker effects on firing rates than the object size, particularly in *monkey H17094.* Sixteen percent of neurons recorded in area 5 (13/83) showed significant differences in firing rates between the left and right rectangles (Table 1). Likewise, the place index comparing the two rectangles (gray curves, Fig. 13) was smaller than the size index, particularly during object manipulation (stages 3–5).

The indices obtained for the individual neurons shown in Figs. 12 and 13 are typical of the population studied. Mean values for the PI, dPI, size and place indices are plotted for

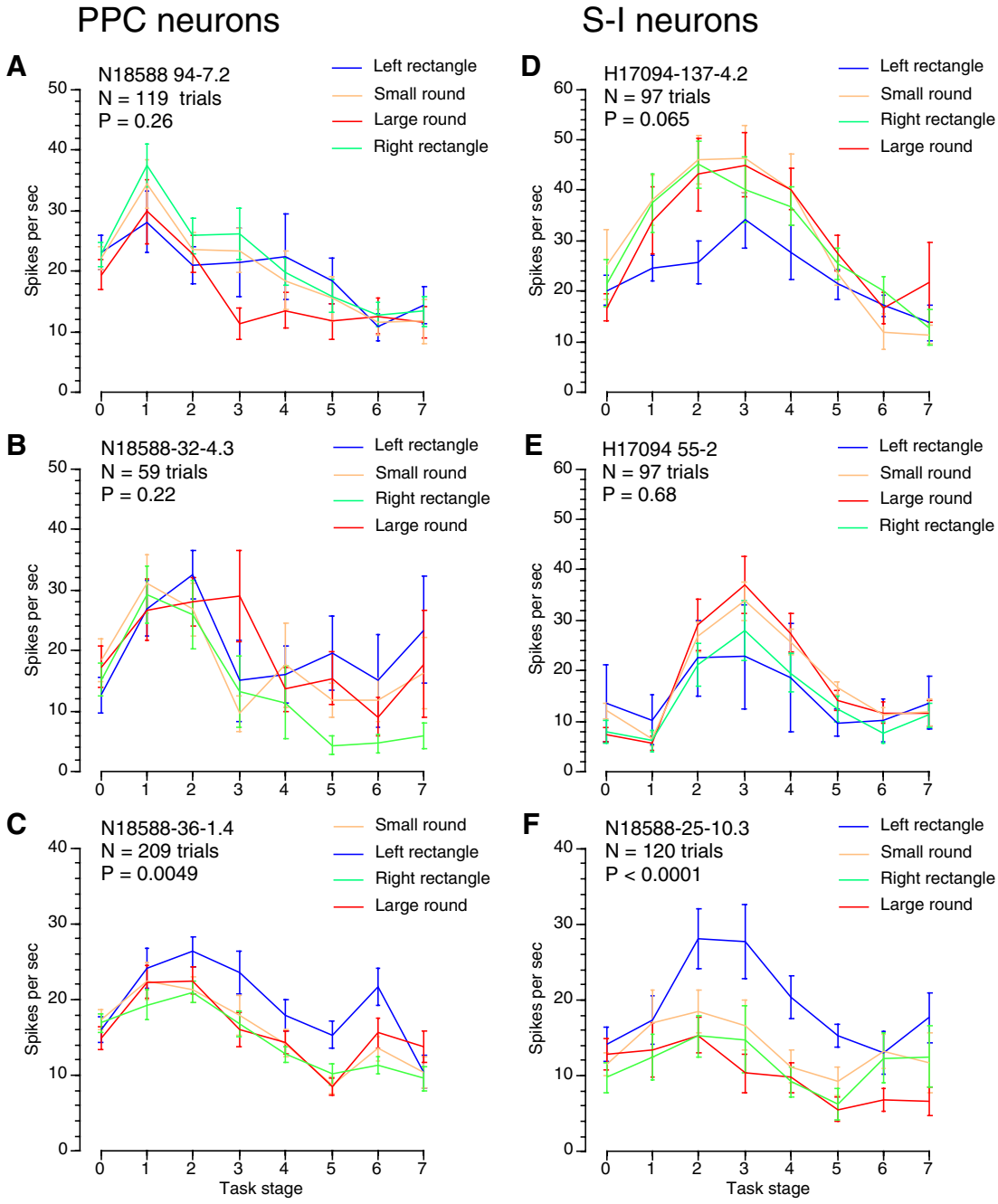

FIG. 10. Average firing rate graphs illustrating the range of object selectivity of neurons recorded in area 5 (*A* and *B*), area 7b/AIP (*C*), and S-I (*F*) of the right hemisphere in *monkey N18588;* same format as Fig. 6. The neurons in *C* and *F* showed significant preferences for the left (medial) rectangle; the area 5 neurons did not distinguish between knobs. Two neurons recorded in S-I in *monkey H17094* are included for comparison (*D* and *E*).

the entire population of 83 neurons in Fig. 14, *B* and *C*. As in the individual examples, the population PI and dPI values were lowest during approach and contact when firing rates were high. Indeed the difference in firing rates between the most and least preferred objects during hand preshaping and initial contact was slightly lower than in the pretrial interval. Mean preference indices increased progressively during the grasp, lift, and hold stages as the hand interacted directly with the object. These findings suggest that tactile feedback from the hand about intrinsic object properties modulated the firing rates of area 5 neurons during manipulatory actions.

The distribution of PI values in the population during each of the task stages is illustrated in Fig. 14*A* by their respective cumulative PIs. The smallest distinction between objects occurred during the approach and contact stages, with median PI values <20; 90% of the neurons tested had PI values <40 in these stages. As in the mean PI graphs, the median PI increased progressively from grasp through lift, hold, and lower actions to 30; the 90th percentile in the lower stage yielded PI values <50.

The population size index reversed as the task progressed. The small round knob was generally favored by higher firing rates during acquisition stages when the hand was preshaped and the

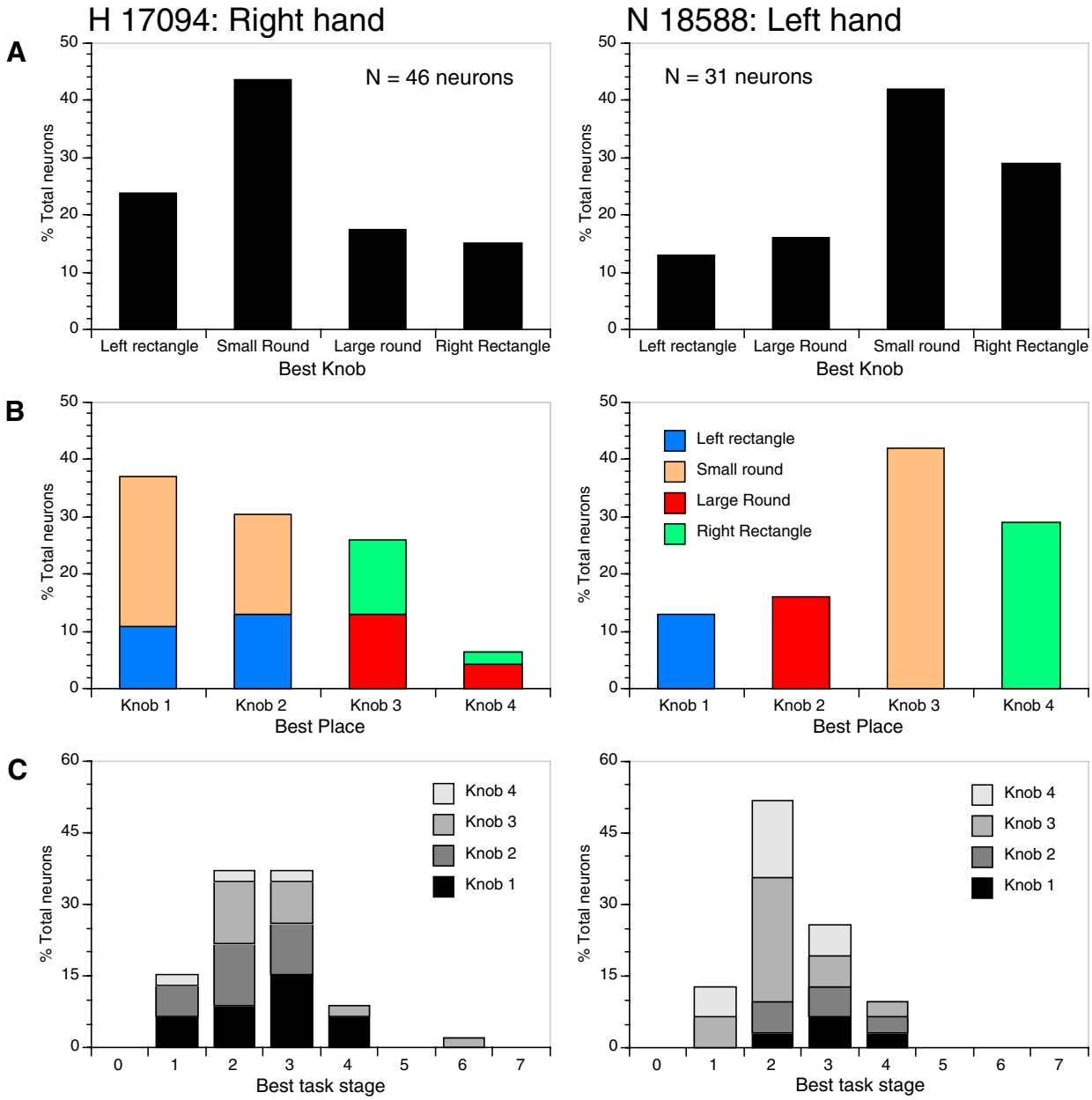

FIG. 11. Population distribution of the objects (*A*), locations (*B*), and task stages (*C*) that yielded the maximum firing rates per stage for the neurons studied. The knobs were shuffled in different recording sessions in *H17094* when testing the right hand; they remained at the indicated places in the recordings from *N18588*. The small sphere was the most preferred object in both animals; it was most likely to evoke peak responses in stage 2 (contact) and at the most medial locations on the shape box.

object grasped. Object preferences shifted during lift and hold when the large round knob evoked stronger responses. The selectivity for the large sphere was most prominent in *monkey N18588,* which used distinctive grasp postures for the large and small spheres.

The population place index indicates that the knob location in the workspace had relatively weak effects on population firing rates. Although the medial rectangle evoked slightly higher firing rates during approach and contact, there was little difference in later stages when firing rates evoked by both objects were low.

Population representation of grasped objects in area 5

To quantify population responses to individual objects, we compiled normalized response profiles for each knob. Four sets of normalized firing rate graphs were computed for each neuron by dividing the mean firing rates per stage to each knob by the peak mean response of the neuron averaged across all trials during the session. The same values were used to normalize responses across neurons in a previous report (Gardner et al. 2007a). Normalized firing rates for each knob were averaged across the population and plotted as a function of task stage in Fig. 15, *left*. The most salient feature of the population curves is the overlap in firing rates evoked by the four knobs during the task. Their temporal profiles of activity rose and fell in parallel, yielding maximum responses at contact. Differences in firing rates between knobs were small in comparison with the changes in mean activity across the task stages.

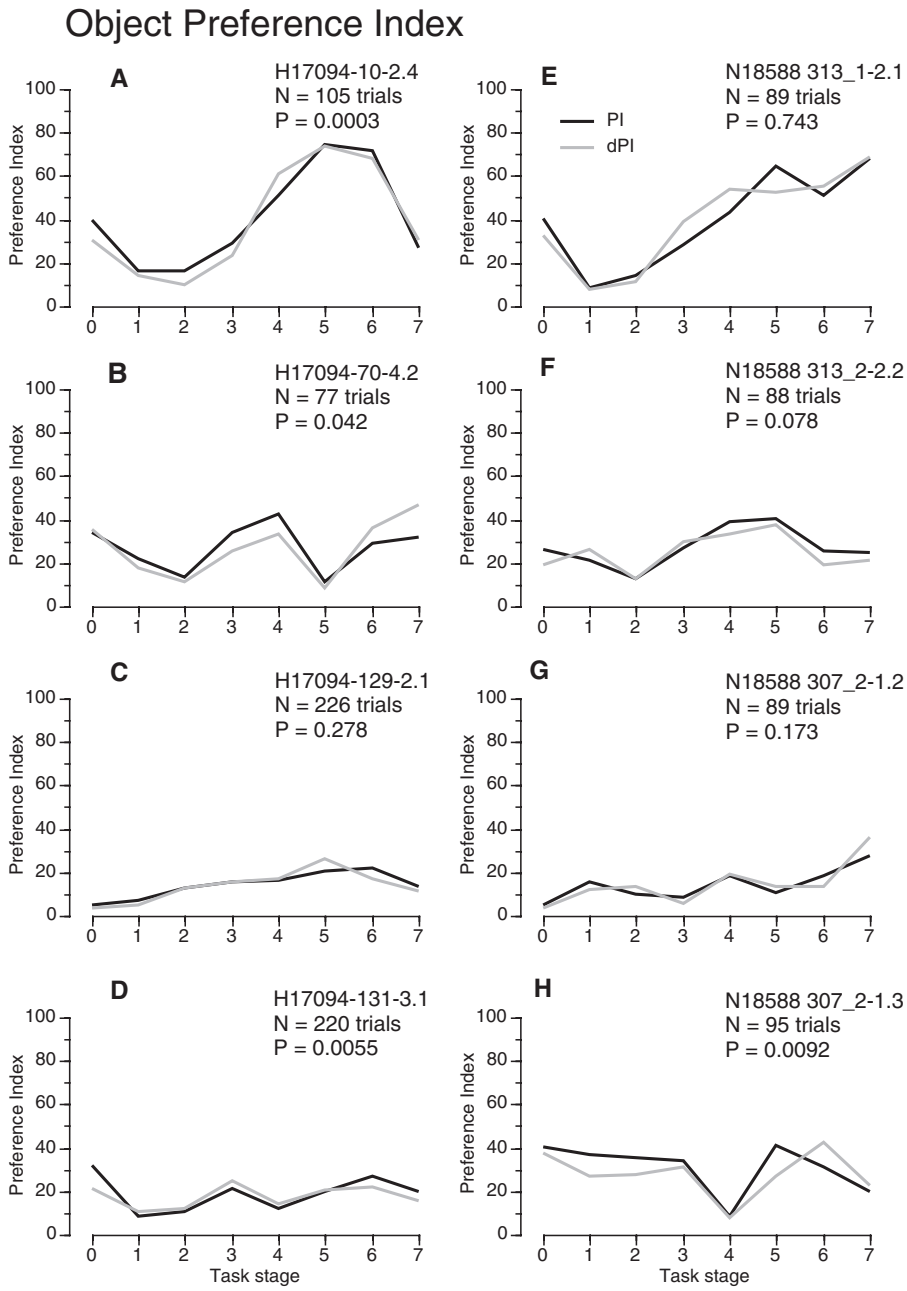

FIG. 12. Place index (PI) and differential place index (dPI) values per stage for the neurons shown in Figs. 6 (*A–D*) and 8 (*E–H*). The indices are lowest in stage 2 when firing rates are maximal and rise in the late stages when firing rates are low. *P* values indicate the selectivity for knobs as determined by repeated-measures ANOVA analyses.

Although the two animals used different hand postures to perform the task, their population response profiles displayed similar contours (Fig. 15, *B* and *C*). The small round knob evoked the highest firing rates during object acquisition (stages 1–3), followed by the medial rectangle (left rectangle when testing the right hand and right rectangle when testing the left hand). The medial rectangle evoked stronger responses than the lateral one during acquisition, but the responses to both rectangles were indistinguishable during lift, hold, and lower stages. The large round knob evoked weaker responses than the small one during acquisition, particularly in *monkey N18588* but produced the highest firing rates during lift and hold in this animal.

We also used a second normalization procedure to assess object selectivity modeled on protocols used by other investigators studying prehension tasks in monkeys (Murata et al. 2000; Raos et al. 2004, 2006; Umilta et al. 2007). Here the mean firing rate per stage for each object was divided by the "best" response—the highest firing rate obtained across all seven task stages and all four test objects (Fig. 11)—and multiplied by 100. The four objects were then ranked from best to worst based on their relative firing rates during the best stage. The normalized mean responses for each rank ordered set were then averaged to compute the population normalized mean rate for the best, second best, third best, and worst knobs.

The rank ordered response profiles in the right column of Fig. 15 show similar selectivity among objects and their associated grasps in area 5 as has been previously demonstrated for neurons in areas F5, F2vr, and M1 (Raos et al. 2004, 2006; Umilta et al. 2007). The spread in responses to the four objects emerged during approach, as the hand was

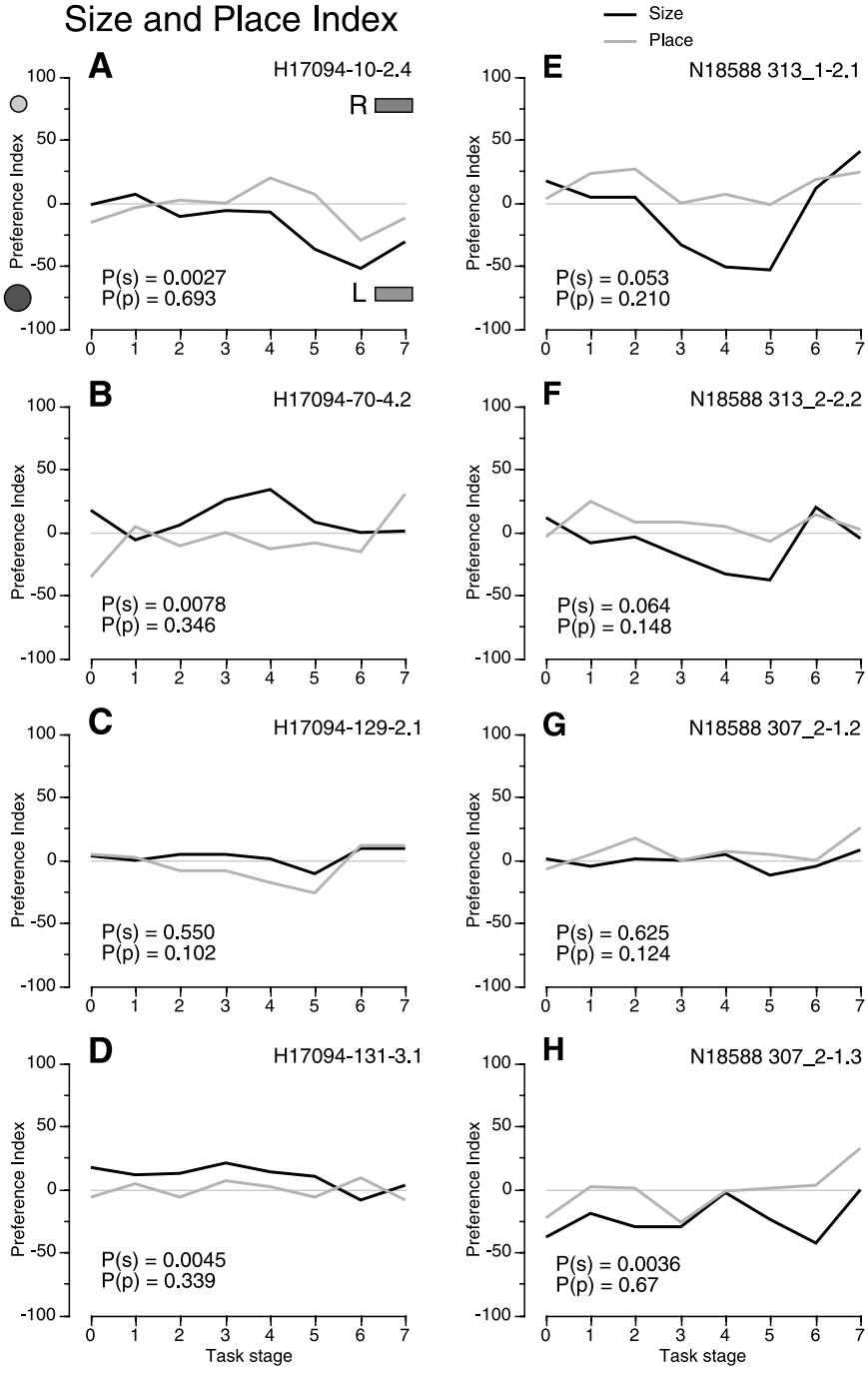

FIG. 13. Size index (black) and place index (gray) per stage for the neurons shown in Figs. 6 (*A–D*) and 8 (*E–H*). Positive values indicate preference for the small sphere (size) and right rectangle (place). *P*(*s*) values indicate the selectivity for size as determined by repeated-measures ANOVA analyses for trials of the large and small spheres. *P*(*p*) values indicate the selectivity for place as determined by repeated-measures ANOVA analyses for trials of the left and right rectangles.

preshaped, and peaked at contact, when direct interaction between the hand and object first occurred. Distinctions between objects persisted as grasp was secured but were progressively reduced during lift, hold, and lower stages. Although responses to the best knob remained distinctive through holding, the firing rates evoked by the other three objects merged during and after lift (stage 4). Note that the peak responses in stage 2 were less than the maximum possible rate because the best responses occurred in different task stages in individual neurons (Fig. 11*C*).

The distribution of rank object preferences provided in Table 3 closely follows the distribution of mean firing rates illustrated in Fig. 15, l*eft*. The representation of individual objects and their associated grasps is distributed nonuniformly across the ensemble, with specific groupings of neurons signaling distinctive objects and actions. The small sphere was the best knob in 42% of the population, followed by the medial rectangle (27%). These two objects each comprised the second best choice for ~30% of area 5 cells. The lateral rectangle was the least preferred object (36%). These findings indicate that neurons in area 5 have distinctive object preferences that are influenced by the object size, shape, and location in the workspace.

DISCUSSION

Hand manipulation neurons that respond to object grasping were first identified in PPC areas 5 and 7 by Mountcastle and

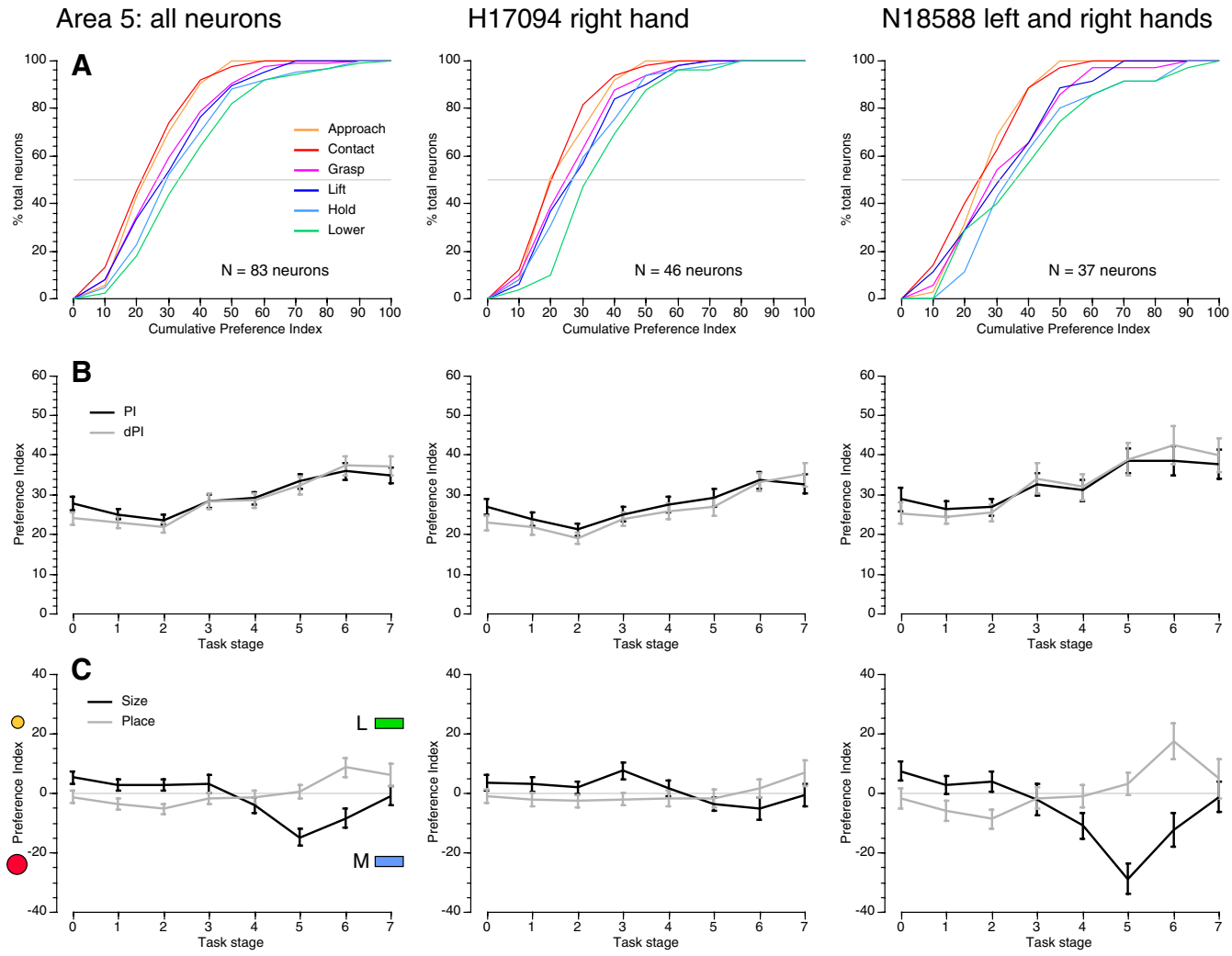

FIG. 14. Population object selectivity in the 2 animals studied; error bars show ± SE per task stage. *A*: cumulative PI values per task stage for the 83 neurons analyzed in area 5. The distribution of PI values in the population was concentrated at low values during approach and contact stages, and rose during manipulatory actions (grasp through lower). *B*: mean PI and dPI averaged across the population paralleled the modal values in *A*. Object preferences were lowest in stage 2 (contact). *C*: mean size and place indices in the 2 animals. The size index was greater than the place index in both animals. The small sphere was favored during acquisition (stages 1–3) and the large 1 during holding (stage 5). The medial rectangle evoked slightly stronger responses during acquisition; the rectangles were indistinguishable in stages 3–5.

co-workers (1975). These cells have been postulated to form part of a "how system" in which action-relevant parameters of objects are encoded to enable performance of skilled tasks (Jeannerod et al. 1995; Milner and Goodale 1995). Recognition of the size, shape, and orientation of objects is important for hand preshaping prior to acquisition and for selection of appropriate grasp postures and hand contact points to accomplish task goals. The relevant information can be provided by visual pathways and/or by tactile inputs from the hand (Jenmalm and Johansson 1997; Jenmalm et al. 1998, 2000, 2003; Johansson et al. 2001). Slowly adapting SA1 fibers innervating Merkel cells in the fingers are the most likely receptors mediating tactile object recognition. They respond parametrically to the curvature of spheres pressed or scanned on the skin with the highest firing rates evoked by objects with the smallest radii (Goodwin and Wheat 2004; Goodwin et al. 1995, 1997; Jenmalm et al. 2003; Johnson and Hsiao 1992; Khalsa et al. 1998; LaMotte and Srinivasan 1987; LaMotte et al. 1998; Srinivasan and LaMotte 1987). The surface curvature of objects grasped in the hand is therefore likely to produce similar modulation of cortical firing rates.

Recordings from neurons in the anterior wall of the intraparietal sulcus (IPS) by Iwamura and co-workers (Iwamura and Tanaka 1978, 1996; Iwamura et al. 1985, 1995) provided evidence that area 5 might serve as a higher-order somatosensory area for shape selectivity. They postulated that area 5 neurons integrated features such as surface curvature and edges to distinguish round and rectangular objects. However, their findings were based on tests of "naturalistic" stimuli and did not use behavioral tasks to quantify neural responses.

The experiments described in this report were designed to test for the first time the effects of object properties on firing patterns of hand manipulation neurons in area 5 when objects were grasped and manipulated in repeated, quantifiable patterns. The main finding of these studies was that the object size and shape had weak modulatory effects on firing rates during task performance. Neural responses rose and fell in parallel

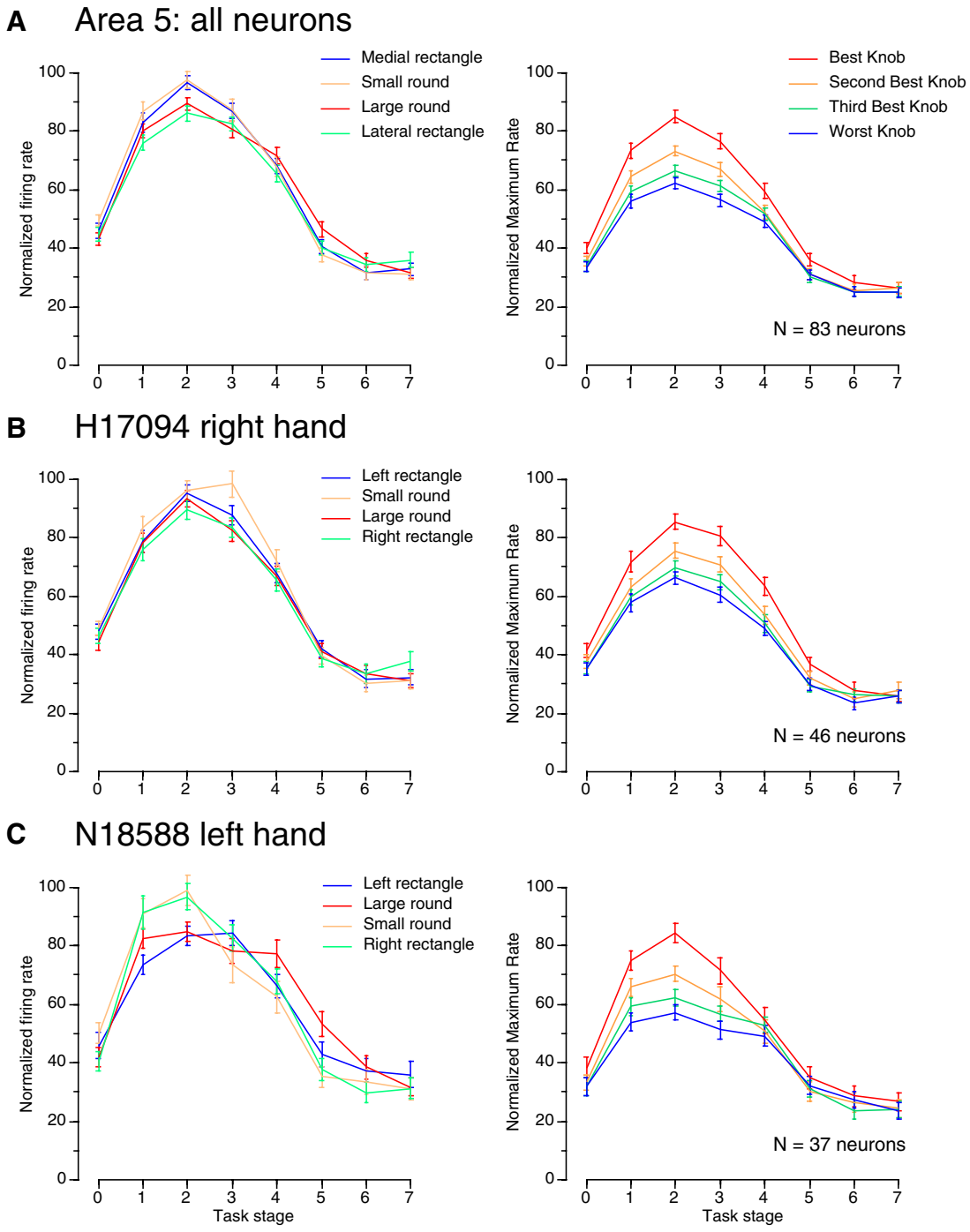

FIG. 15. Population object selectivity in the 2 animals studied; error bars show ± SE per task stage. *Left*: firing rates of each neuron were normalized by the peak mean response across all trials and plotted as a function of the knob tested. *Right*: responses normalized by the maximum response evoked across all knobs and stages and grouped as a function of rank object preference in the "best" stage. *A*: mean normalized firing rate per task stage for all of the neurons tested in this study. Object selectivity was less prevalent in *monkey H17094,* but the small sphere evoked the highest rates in both animals. *B* and *C*: mean normalized firing rates in the left hemisphere of *monkey H17094* (*B*) and the right hemisphere of *monkey N18588* (*C*).

with the hand actions as the task progressed from acquisition to manipulation and release of grasp. However, only 34% of the population tested showed statistically significant modulation of firing rates related to the object's shape, size, or location. Object-linked differences in firing rates were small in comparison with the changes in mean activity across task stages. Selectivity for particular objects, when present, was characterized by amplitude modulation of firing rates following hand contact and differences in response duration as the object was manipulated. Objects that were grasped with the same hand postures evoked similar responses in area 5 neurons, regardless of whether their surface was curved or flat or where they were located in the workspace.

Unlike visuomotor neurons in area AIP (Murata et al. 1996, 2000), none of the cells tested in area 5 responded selectively to only one object class nor did we find cells that were

TABLE 3. *Rank object preference in area 5*

	Small Round		Large Round		Medial Rectangle		Lateral Rectangle	
Area 5 (83)	Total	Percent	Total	Percent	Total	Percent	Total	Percent
Best knob	35	42.2	13	15.7	22	26.5	13	15.7
Second best	25	30.1	12	14.4	26	31.3	20	24.1
Third best	9	10.8	33	39.8	21	25.3	20	24.1
Worst knob	14	16.9	25	30.1	14	16.9	30	36.1

Number of cells is in parentheses.

unresponsive to grasp of one object type alone. However, Murata and co-workers tested a wider variety of objects that required greater diversity of hand postures to be grasped. It is therefore possible that object selectivity might occur more frequently in area 5 if tested with objects other than spheres or rectangular blocks.

Rank-ordered preferences for specific objects emerged in the population during approach as the hand was preshaped for grasping. The greatest spread in firing rates between the most and least preferred objects occurred at contact when the object was secured in the hand and during static grasp. Responses converged in the later task stages when the objects were lifted and held. Individual neurons often showed distinct preferences for particular objects, but the selectivity was distributed non-uniformly in the population. Forty-three percent of the neurons studied responded most vigorously to the small sphere. This object was held in a semi-precision grip between the thumb and digits 2 and 3 or with a tightly flexed whole hand grasp. The three larger objects were held in a power grasp by the entire hand. The digits were extended along the flat face(s) of the rectangular blocks or flexed around the circumference of the large sphere. Acquisition responses were stronger when objects were placed at medial locations in the workspace, especially sites near the midline of the animal's body, than at positions lateral to the shoulder. The distinctions based on workspace location disappeared in later stages. During the lift and hold stages, the most preferred object was the large sphere, apparently because it was the heaviest object tested, and required greater load forces to accomplish the task goals.

Our findings differ somewhat from earlier reports by Iwamura and co-workers that neurons in area 5 responded selectively to one class of objects but not to others (Iwamura and Tanaka 1978, 1996; Iwamura et al. 1985, 1995). We believe that the discrepancy between our results and theirs may be due to methodological factors. The test objects used in our study differed in size, shape, weight, and location in the workspace but were all made of metal and therefore had the same compliance. They were all simultaneously visible or blocked from view and therefore had no distinguishing salience beyond their relevance to reward on particular trials. The studies by Iwamura and co-workers were based on single trial observations when a monkey's hand was placed on a variety of common objects such as fruits, rulers, wooden blocks, or brushes. The animals were not trained to do anything in particular with the objects, but one can imagine that these items might have very different behavioral significance to them. It is possible that the selectivity for shape described in their studies may actually reflect the animal's intentions or interest in the test objects. It is clear from Mountcastle's original observations (Mountcastle et al. 1975) that the intentions motivating grasp of food are different from those directed toward inedible wooden objects. Alternatively, the shape selectivity reported in the Iwamura and Tanaka studies may reflect differences in hand postures and distinctive muscle activation patterns used by their animals to grasp the various test objects (Brochier et al. 2004).

The task goals in our paradigm were to manipulate objects in a particular fashion (lift them). The animals were not required to discriminate shape, although they may have used shape cues during approach to distinguish objects when they did not look directly at them. In fact the cues delivered on each trial signaled only the location of the rewarded object not its shape (see Fig. 1*A*). Therefore it is possible that greater object selectivity might be revealed in area 5 if object shape and/or size cues were relevant features of the task, requiring the animal to locate a matching object.

Interaction of object features with hand kinematics during prehension

The orientation of the hand during approach and the selection of specific grasp points by the fingers are flexible and can be readily adapted to task requirements. Objects can be grasped in a variety of ways depending on their physical properties, such as size and shape, the context in which they are acquired, and the goal of the grasping action (Ansuini et al. 2006; Castiello 2005; Mason et al. 2001, 2004; Roy et al. 2002; Santello et al. 1998, 2002). A pen may be grasped differently if the goal is writing or passing it to someone else. Conversely, different objects can be grasped in the same manner when they are similar in size, and the task goals are comparable. In our task, the goal was lifting objects, and not surprisingly, each of the animals devised a common personal task strategy that allowed them to perform this action efficiently, regardless of which particular object was cued on a trial. The standardized behavioral strategy was expressed as similar grasp postures used for each object over the period of study and reproducible timing of task stages during the critical actions needed for reward. The fact that we did not record strong distinctions between objects in area 5 suggests that these neurons may represent the goal of the hand behaviors—grasping—rather than the specific object that is grasped. Recent fMRI studies suggest that neurons in the anterior intraparietal sulcus (aIPS) of humans also play a significant role in the representation of action plans and goals during grasping (Binkofski et al. 1998, 1999; Cavina-Pratesi et al. 2004; Culham et al. 2003; Ehrsson et al. 2000, 2001, 2003; Frey et al. 2005; Hamilton and Grafton 2006; Shikata et al. 2003; Shmuelof and Zohary 2006).

Studies of whole hand kinematics during reach-to-grasp tasks in humans (Mason et al. 2001; Santello et al. 1998, 2002)

and monkeys (Mason et al. 2004; Theverapperuma et al. 2006) indicate that 80–90% of the total behavioral variance between objects can be described by two principal components or eigenpostures: *1*) an open hand posture with the metacarpal-phalangeal (MCP) and proximal interphalangeal (PIP) joints in mid-flexion and *2*) a hyperextended and abducted posture of the MCPs and PIPs. These authors posit that the CNS can simplify acquisition behaviors for different objects by variation in the amplitude and timing of the two components. The major changes in hand kinematics in their analyses occurred just before and after contact and were governed by tactile cues and previous experience with the objects. Higher-order components specific to individual objects allowed further refinement of grasping behaviors as skills were learned and refined.

The emphasis on common hand synergies during reaching may explain our observations that the neural representations of the test objects overlapped during much of the approach interval. Responses diverged at the end of the approach stage just prior to contact and during hand positioning as it slid into place to secure the grasp. The tactile feedback during movement of the hand over the object surface simplified the formation of grasp as the animals used their fingertips to trace the object contours until the chosen grip site was secured. The question therefore arises as to whether objects are represented in area 5 in terms of the hand postures needed to grasp and manipulate them or in terms of their intrinsic tactile and visual features—size, shape, orientation, and texture. The answer is by no means clear as there is much ambiguity in the data from our studies as well as from earlier investigations of parieto-frontal networks engaged in prehension tasks.

Parieto-frontal circuits engaged in prehension

Neural responses during grasping could be related to intrinsic object properties, the area of tactile contact on the skin, or the particular hand postures used by the animals. In this regard, it is instructive to consider previous single neuron studies in which monkeys grasped a variety of objects (Murata et al. 1996, 1997, 2000; Raos et al. 2004, 2006; Rizzolatti and Luppino 2001; Sakata et al. 1995, 1997; Taira et al. 1990; Umilta et al. 2007). These authors proposed that neurons in areas AIP, F5, F2vr, and M1 represent objects by the hand postures needed to grasp them or by the underlying patterns of muscle activation. Neurons comprising these parieto-frontal circuits are postulated to perform sensorimotor transformations of visual properties of objects into a matching hand posture that mimics the object's shape, allowing it to be grasped and manipulated efficiently (Jeannerod et al. 1995; Rizzolatti and Luppino 2001).

There are striking similarities between our findings and theirs, particularly with regard to the responses of motor dominant and visuomotor nonobject neurons in areas AIP and F5. Half of these AIP cells were described as selective for common patterns of handgrip, such as the precision grasp used to manipulate small spheres, cubes and cones. Another 25% of this population was highly selective for objects that were grasped with unique grip styles, and the remainder did not distinguish between the test objects. Murata et al. (2000) concluded that such neurons "appeared to be selective for the pattern of the handgrip rather than for the object itself" because they responded only to direct engagement between the hand and the object. Consequently, their firing patterns were thought to represent "the shape of the handgrip, grip size, or hand orientation."

Although visuomotor neurons in area AIP may identify the type of grasp that is required to perform prehension tasks, the motor areas of the frontal lobe are thought to select the muscle groups and patterns of motor synergies needed to accomplish the task goals. These include areas F5, F2vr, and M1. F5 neurons show greater selectivity for particular objects and their associated grasp styles than simultaneously recorded M1 neurons (Umilta et al. 2007). The strongest distinctions occurred at contact and during grasping; object preferences decreased during pull and hold periods (Raos et al. 2006; Umilta et al. 2007). Similarly, neurons in M1 cortex were most likely to distinguish between individual objects following hand contact and during grasping. These are precisely the same intervals in which area 5 neurons in our study were most likely to distinguish between individual knobs. These findings suggest that somatosensory input from the hand after contact provides powerful signals of object properties and grasp actions to neurons in both parietal and frontal cortex.

By analogy with these studies, it appears that neurons in area 5 may represent the grasping actions that are planned during prehension tasks in terms of the motor synergies needed to accomplish the task goals, as well as the object properties perceived by the sense of touch. This dual role suggests that objects are represented in area 5, as in area AIP, in hand-centered coordinates. Both sets of PPC neurons are engaged in sensorimotor transformations of visually or tactually perceived object properties into a pattern of hand muscle synergies needed to accomplish the task goals. The object size and shape define the opposition space between the thumb and the fingers during hand preshaping, and the type of grip used once contact is established. Sensory feedback from the hand signals the accomplishment of grasping and manipulatory actions when successful and is used for error correction when they fail to achieve the desired goals.

The timing of area 5 responses presented in this report suggests that the early neural activity during approach encodes the action plans, but later responses include sensory feedback concerning ongoing, self-generated behaviors. They support the notion that PPC neurons are engaged in on-line correction of planned actions, integrating efference copy of the motor commands with sensory feedback during actual performance (Andersen and Buneo 2002; Buneo and Andersen 2006; Crammond and Kalaska 1989; Fogassi and Luppino 2005; Gardner 2007; Gardner et al. 2007a,b; Glover et al. 2005; Jeannerod 1994; Jeannerod et al. 1995; Kalaska et al. 1997; Rice et al. 2006; Sakata et al. 1997; Tunik et al. 2005, 2007).

In their pioneering studies, Mountcastle and co-workers (1975) stressed the importance of motor intentionality and goal-directed actions of the hand and arm in determining the firing rates of PPC neurons. When objects such as the knobs used in our prehension task are acquired for use as tools, the goal is to stabilize them in the hand and to minimize tangential movements. In this manner, hand and object move as a unit to perform the intended action. Hand contact with the wrong object, or unintended slippage in the hand, are recognized by tactile signals that are used to correct the behavior, by redirecting the reach, or increasing the grip force.

Neuroanatomical evidence suggests that area 5 may provide somatosensory information about hand actions to area AIP and receives reciprocal connections from this region (Neal et al. 1986; Selzer and Pandya 1980). In addition, hand manipulation neurons in area 5 may provide somatosensory information about hand shape prior to and during prehension to area F2vr, the hand representation zone in dorsal premotor cortex (Marconi et al. 2001; Matelli et al. 1998; Raos et al. 2003). The large population of motor dominant neurons in area F2vr (Raos et al. 2003, 2004) may be engaged in reciprocal feed-forward and feedback circuits with area 5. The similarity of prehension task responses in their studies and ours supports such a functional linkage.

Anatomical connectivity between area 5 and dorsal premotor cortex may play a role in temporal synchronization of reach and grasp behaviors (Chieffi and Gentilucci 1993; Paulignan and Jeannerod 1996; Wise et al. 1997). Kinematic studies of prehension in humans and monkeys have demonstrated that reach and hand preshaping times are generally longer for small objects because of the greater precision of hand positioning required for grasping them (Gentilucci et al. 1991; Marteniuk et al. 1990; Roy et al. 2002). Similarly, we observed longer duration acquisition times for the small sphere than for the other three objects (Table 2). Interestingly, small objects grasped between the fingers with a precision grip were most likely to evoke the strongest responses in our area 5 populations, as well as in other regions of the parieto-frontal prehension network (Murata et al. 2000; Raos et al. 2004, 2006; Umilta et al. 2007). The preference for the small sphere by 43% of the neurons studied in area 5 suggests that accuracy of hand positioning on objects is a crucial component of their physiological function. Importantly, activation of the human homologue of area AIP (area aIPS) in functional imaging studies was more intense when the subjects grasped small spheres in a precision grip than when large spheres were held in a whole hand grasp (Begliomini et al. 2007). These authors suggested that greater mobilization of cortical resources was required to grasp and manipulate small objects, particularly in area aIPS.

Functional role of area 5 during prehension in humans

Clinical studies of patients with lesions to the posterior parietal cortex revealed severe disturbances of complex tactile sensitivity and astereognosis (Binkofski et al. 2001; Pause and Freund 1989; Pause et al. 1989). These lesions were characterized by motor deficits, particularly problems with precision grip, force control, manipulatory behaviors, and a paucity of exploratory finger movements. This syndrome was named *tactile apraxia* (Binkofski et al. 2001) because of the loss of purposive, goal-directed motor behaviors of the hand.

Similar deficits in on-line control of grasping have been elicited transiently in humans in studies using transcranial magnetic stimulation (TMS) applied to the anterior end of the IPS. TMS pulses interfered with adjustments in grip aperture during task execution but not during task planning when applied to the superior parietal lobule (Glover et al. 2005) as well as to the inferior parietal lobule (Rice et al. 2006; Tunik et al. 2005, 2007). Glover et al. (2005) note that while most of these studies have focused on sites in the IPL (BA40), "it is clear that the critical area [for on-line control of grasping] consistently surrounds the IPS."

Likewise, functional imaging studies of active hand movements have focused primarily on area aIPS centered in the IPL near the junction of the postcentral and intraparietal sulci (Binkofski et al. 1998, 1999; Culham et al. 2003; Frey et al. 2005; Grefkes et al. 2002). Although these authors have stressed the importance of area aIPS in grasping tasks, there is considerable evidence in both their data and that of other investigators for an important focus of activity in the anterior SPL (human BA5) during object manipulation (Binkofski et al. 1998, 1999; Bodegård et al. 2001; Cavina-Pratesi et al. 2007; Culham et al. 2003; Stoeckel et al. 2004; Wenderoth et al. 2006). Anterior SPL neurons in the human brain showed enhanced activity during tactile exploration when visual guidance was absent, and the subjects needed to rely on somatosensory feedback for controlling hand movements. Stoeckel et al. (2004) noted that the anterior SPL comprises an important component of the parietal-premotor circuit activated during hand manipulation of three-dimensional objects. Likewise, Binkofski and co-workers (1999) noted that neurons in anterior SPL (called area PG) and the secondary somatic sensory cortex (SII) are both involved in controlling exploratory manipulation, but serve different roles. They state: "SII and the adjacent areas describe the objects in terms of their intrinsic (physical) properties. In contrast, PE and the adjacent areas (superior parietal stream) describe the objects in terms of hand postures necessary to interact with them. The functional role of SII is therefore to capture information from the external world, whereas that of PE is to describe the same objects from an internal (kinesthetic) point of view." These ideas are consistent with our proposal that neural activity in area 5 may represent self-generated hand actions, aiding subjective awareness of the success or failure of active touch and other voluntary hand movements (Gardner et al. 2007a).

The data presented in our report support hypotheses of parallel processing of hand actions and tactile information that allow humans and non-human primates to interact with objects in their environment in purposeful ways to accomplish a variety of goals. The studies demonstrate the flexibility of neural control when task goals require performance of a particular action with similarly shaped tools. Monkeys and humans are able to adapt their behavior to use simple motor schemas to accomplish a particular action efficiently and smoothly, ignoring details such as object form when they are unnecessary for achieving the task goals.

ACKNOWLEDGMENTS

We thank Dr. Daniel J. Debowy for many contributions to these studies, J. Bailey Kohlenstein, A. Brown, A. Hall, A. Harris, M. Herzlinger, C. Kops, M. Natiello and I. Simanovich for skilled technical support and A. Barzack and P. Pearce for assistance with the statistical analyses. We are most appreciative of the collaborative efforts of Dr. Edward G. Jones in histological analyses of one of the animals used in this study; 3-D reconstructions from frozen block face images of the brain can be found at his website www.brainmaps.org. We are grateful to Drs. Daniel Gardner, Michael E. Goldberg, Eric Lang, Rodolfo Llinás, and John I. Simpson for many helpful comments and criticisms of earlier versions of this report.

Present addresses: K. Srinivasa Babu, Dept. of Neurological Sciences, Christian Medical College, Vellore—632 004, India; S. Ghosh, Centre for Neuromuscular and Neurological Disorders, University of Western Australia, Queen Elizabeth II Medical Centre, Nedlands, Perth, Western Australia 6009.

GRANTS

Major funding for this study has been provided by National Institutes of Health Grant R01 NS-11862 and Grant R01 NS-44820.

REFERENCES

Andersen RA, Buneo CA. Intentional maps in posterior parietal cortex. *Annu Rev Neurosci* 25: 189–220, 2002.

Ansuini C, Santello M, Massaccesi S, Castiello U. Effects of end-goal on hand shaping. *J Neurophysiol* 95: 2456–2465, 2006.

Begliomini C, Wall MB, Smith AT, Castiello U. Differential cortical activity for precision and whole-hand visually guided grasping in humans. *Eur J Neurosci* 25: 1245–1252, 2007.

Binkofski F, Buccino G, Stephan KM, Rizzolatti G, Seitz RJ, Freund HJ. A parieto-premotor network for object manipulation: evidence from neuroimaging. *Exp Brain Res* 128: 210–213, 1999.

Binkofski F, Dohle C, Posse S, Stephan K, Hefter H, Seitz R, Freund HJ. Human anterior intraparietal area subserves prehension: a combined lesion and functional MRI activation study. *Neurology* 50: 1253–1259, 1998.

Binkofski F, Kunesch E, Classen J, Seitz RJ, Freund HJ. Tactile apraxia: unimodal apractic disorder of tactile object exploration associated with parietal lobe lesions. *Brain* 124: 132–144, 2001.

Bodegård A, Geyer S, Grefkes C, Zilles K, Roland PE. Hierarchical processing of shape in the human brain. *Neuron* 31: 317–328, 2001.

Brochier T, Spinks R, Umilta MA, Lemon RN. Patterns of muscle activity underlying object-specific grasp by the macaque monkey. *J Neurophysiol* 92: 1770–1782, 2004.

Buneo CA, Andersen RA. The posterior parietal cortex: sensorimotor interface for the planning and online control of visually guided movements. *Neuropsychologia* 44: 2594–2606, 2006.

Castiello U. The neuroscience of grasping. *Nat Rev Neurosci* 6: 726–736, 2005.

Cavina-Pratesi C, Goodale MA, Culham JC. FMRI reveals a dissociation between grasping and perceiving the size of real 3D objects. *PloS ONE* 2: e424, 2007.

Chieffi S, Gentilucci M. Coordination between the transport and the grasp component during prehension movements. *Exp Brain Res* 94: 471–477, 1993.

Crammond DJ, Kalaska JF. Neuronal activity in primate parietal cortex area 5 varies with intended movement direction during an instructed-delay period. *Exp Brain Res* 76: 458–462, 1989.

Culham JC, Danckert SL, DeSouza JF, Gati JS, Menon RS, Goodale MA. Visually guided grasping produces fMRI activation in dorsal but not ventral stream brain areas. *Exp Brain Res* 153: 180–189, 2003.

Debowy DJ, Babu KS, Hu EH, Natiello M, Reitzen S, Chu M, Sakai J, Gardner EP. New applications of digital video technology for neurophysiological studies of hand function. In: *The Somatosensory System: Deciphering the Brain's Own Body Image,* edited by Nelson R. Boca Raton FL: CRC, 2002, p. 219–241.

Debowy DJ, Ghosh S, Ro JY, Gardner EP. Comparison of neuronal firing rates in somatosensory and posterior parietal cortex during prehension. *Exp Brain Res* 137: 269–291, 2001.

de Lafuente V, Romo R. Neural correlate of subjective sensory experience gradually builds up across cortical areas. *Proc Natl Acad Sci USA* 103: 14266–14371, 2006.

Ehrsson HH, Fagergren E, Forssberg H. Differential fronto-parietal activation depending on force used in a precision grip task: an fMRI study. *J Neurophysiol* 85: 2613–2623, 2001.

Ehrsson HH, Fagergren A, Johansson RS, Forssberg H. Evidence for the involvement of the posterior parietal cortex in coordination of fingertip forces for grasp stability in manipulation. *J Neurophysiol* 90: 2978–2986, 2003.

Ehrsson HH, Fagergren A, Jonsson T, Westling G, Johansson RS, Forssberg H. Cortical activity in precision- versus power-grip tasks: an fMRI study. *J Neurophysiol* 83: 528–536, 2000.

Fogassi L, Luppino G. Motor functions of the parietal lobe. *Curr Opin Neurobiol* 15: 626–631, 2005.

Frey SH, Vinton D, Norlund R, Grafton ST. Cortical topography of human anterior intraparietal cortex active during visually guided grasping. *Cogn Brain Res* 23: 397–405, 2005.

Gardner EP. Dorsal and ventral streams in the sense of touch. In: *The Senses: A Comprehensive Reference. Somatosensation*, edited by Gardner EP, Kaas JH. Oxford: Elsevier, 2007, vol. 5. In press.

Gardner EP, Babu KS, Reitzen SD, Ghosh S, Brown AM, Chen J, Hall AL, Herzlinger MD, Kohlenstein JB, Ro JY. Neurophysiology of prehension. I. Posterior parietal cortex and object-oriented hand behaviors. *J Neurophysiol* 97: 387–406, 2007a.

Gardner EP, Debowy D, Ro JY, Ghosh S, Babu KS. Sensory monitoring of prehension in the parietal lobe: a study using digital video. *Behav Brain Res* 135: 213–224, 2002.

Gardner EP, Ro JY, Debowy D, Ghosh S. Facilitation of neuronal firing patterns in somatosensory and posterior parietal cortex during prehension. *Exp Brain Res* 127: 329–354, 1999.

Gardner EP, Ro JY, Babu KS, Ghosh S. Neurophysiology of prehension. II. Response diversity in primary somatosensory (S-I) and motor (M-I) cortices. *J Neurophysiol* 97: 1656–1670, 2007b.

Gentilucci M, Castiello U, Corradini ML, Scarpa M, Umilta C, Rizzolatti G. Influence of different types of grasping on the transport component of prehension movements. *Neuropsychologia* 29: 361–378, 1991.

Glover S, Miall RC, Rushworth FS. Parietal rTMS disrupts the initiation but not the execution of on-line adjustments to a perturbation of object size. *J Cogn Neurosci* 17: 124–136, 2005.

Goodwin AW, Browning AS, Wheat HE. Representation of curved surfaces in responses of mechanoreceptive afferent fibers innervating the monkey's fingerpad. *J Neurosci* 15: 798–810, 1995.

Goodwin AW, Macefield VG, Bisley JW. Encoding of object curvature by tactile afferents from human fingers. *J Neurophysiol* 78: 2881–2888, 1997.

Goodwin AW, Wheat HE. Sensory signals in neural populations underlying tactile perception and manipulation. *Annu Rev Neurosci* 27: 53–77, 2004.

Grefkes C, Weiss PH, Zilles K, Fink GR. Crossmodal processing of object features in human anterior intraparietal cortex: an fMRI study implies equivalencies between humans and monkeys. *Neuron* 35: 173–184, 2002.

Hamilton AF, Grafton ST. Goal representation in human anterior intraparietal sulcus. *J Neurosci* 26: 1133–1137, 2006.

Iwamura Y, Tanaka M. Postcentral neurons in hand region of area 2: their possible role in the form discrimination of tactile objects. *Brain Res* 150: 662–666, 1978.

Iwamura Y, Tanaka M. Representation of reaching and grasping in the monkey postcentral gyrus. *Neurosci Lett* 214: 147–150, 1996.

Iwamura Y, Tanaka M, Hikosaka O, Sakamoto M. Postcentral neurons of alert monkeys activated by the contact of the hand with objects other than the monkey's own body. *Neurosci Lett* 186: 127–130, 1995.

Iwamura Y, Tanaka M, Sakamoto M, Hikosaka O. Functional surface integration, submodality convergence, and tactile feature detection in area 2 of the monkey somatosensory cortex. *Exp Brain Res* 10: 44–58, 1985.

Jeannerod M. The hand and the object: the role of posterior parietal cortex in forming motor representations. *Can J Physiol Pharmacol* 72: 535–541, 1994.

Jeannerod M, Arbib MA, Rizzolatti G, Sakata H. Grasping objects: the cortical mechanisms of visuomotor transformation. *Trends Neurosci* 18: 314–320, 1995.

Jenmalm P, Johansson RS. Visual and somatosensory information about object shape control manipulative fingertip forces. *J Neurosci* 17: 4486–4499, 1997.

Jenmalm P, Birznieks I, Goodwin AW, Johansson RS. Influence of object shape on responses of human tactile afferents under conditions characteristic of manipulation. *Eur J Neurosci* 18: 164–176, 2003.

Jenmalm P, Dahlstedt S, Johansson RS. Visual and tactile information about object-curvature control fingertip forces and grasp kinematics in human dextrous manipulation. *J Neurophysiol* 84: 2984–2997, 2000.

Jenmalm P, Goodwin AW, Johansson RS. Control of grasp stability when humans lift objects with different surface curvatures. *J Neurophysiol* 79: 1643–1652, 1998.

Johansson RS. Sensory control of dexterous manipulation in humans. In: *Hand and Brain,* edited by Wing AM, Haggard P, Flanagan JR. San Diego CA: Academic, 1996, p. 381–414.

Johansson RS, Cole KJ. Sensory-motor coordination during grasping and manipulative actions. *Curr Opin Neurobiol* 2: 815– 823, 1992.

Johansson RS, Westling G, Backstrom A, Flanagan JR. Eye-hand coordination in object manipulation. *J Neurosci* 21: 6917–6932, 2001.

Johnson KO, Hsiao SS. Neural mechanisms of tactual form and texture perception. *Annu Rev Neurosci* 15: 227–250, 1992.

Kalaska JF, Caminiti R, Georgopoulos AP. Cortical mechanisms related to the direction of two-dimensional arm movements: relations in parietal area 5 and comparison with motor cortex. *Exp Brain Res* 51: 247–260, 1983.

Kalaska JF, Scott SH, Cisek P, Sergios LE. Cortical control of reaching movements. *Curr Opin Neurobiol* 7: 849–859, 1997.

Khalsa PS, Friedman RM, Srinivasan MA, LaMotte RH. Encoding of shape and orientation of objects indented into the monkey fingerpad by populations of slowly and rapidly adapting mechanoreceptors. *J Neurophysiol* 79: 3238–3251, 1998.

LaMotte RH, Friedman RM, Lu C, Khalsa PS, Srinivasan MA. Raised object on a planar surface stroked across the fingerpad: responses of cutaneous mechanoreceptors to shape and orientation. *J Neurophysiol* 80: 2446–2466, 1998.

LaMotte RH, Srinivasan MA. Tactile discrimination of shape: responses of slowly adapting mechanoreceptive afferents to a step stroked across the monkey fingerpad. *J Neurosci* 7: 1655–1671, 1987.

Marconi B, Genovesio A, Battaglia-Mayer A, Ferraina S, Squatrito S, Molinari M, Lacquaniti F, Caminiti R. Eye-hand coordination during reaching. I. Anatomical relationships between parietal and frontal cortex. *Cereb Cortex* 11: 513–527, 2001.

Marteniuk RG, Leavitt JL, MacKenzie CL, Athenes S. Functional relationships between grasp and transport components in a prehension task. *Hum Mov Sci* 9: 149–176, 1990.

Mason CR, Gomez JE, Ebner TJ. Hand synergies during reach-to-grasp. *J Neurophysiol* 86: 2896–2910, 2001.

Mason CR, Theverapperuma LS, Hendrix CM, Ebner TJ. Monkey hand postural synergies during reach-to-grasp in the absence of vision of the hand and object. *J Neurophysiol* 91: 2826–2837, 2004.

Matelli M, Govoni P, Galletti C, Kutz DF, Luppino G. Superior area 6 afferents from the superior parietal lobule in the macaque monkey. *J Comp Neurol* 402: 327–352, 1998.

Milner AD, Goodale MA. *The Visual Brain in Action.* Oxford, UK: Oxford Univ. Press, 1995.

Mountcastle VB, Lynch JC, Georgopoulos A, Sakata H, Acuna C. Posterior parietal association cortex of the monkey: command functions for operations within extrapersonal space. *J Neurophysiol* 38: 871–908, 1975.

Murata A, Fadiga L, Fogassi L, Gallese V, Raos V, Rizzolatti G. Object representation in the ventral premotor cortex (area F5) of the monkey. *J Neurophysiol* 78: 2226–2230, 1997.

Murata A, Gallese V, Kaseda M, Sakata H. Parietal neurons related to memory-guided hand manipulation. *J Neurophysiol* 75: 2180–2186, 1996.

Murata A, Gallese V, Luppino G, Kaseda M, Sakata H. Selectivity for the shape, size and orientation of objects for grasping in neurons of monkey parietal area AIP. *J Neurophysiol* 83: 2580–2601, 2000.

Neal JW, Pearson RCA, Powell TPS. The organization of the corticocortical projection of area 5 upon area 7 in the parietal lobe of the monkey. *Brain Res* 381: 164–167, 1986.

Pandya DN, Seltzer B. Intrinsic connections and architectonics of posterior parietal cortex in the rhesus monkey. *J Comp Neurol* 204: 196–210, 1982.

Paulignan Y, Jeannerod M. Prehension movements: The visuomotor channels hypothesis revisited. In: *Hand and Brain*, edited by Wing AM, Haggard P, Flanagan JR. San Diego, CA: Academic, 1996, p. 265–282.

Pause M, Freund H-J. Role of the parietal cortex for sensorimotor transformation. Evidence from clinical observations. *Brain Behav Evol* 33: 136–140, 1989.

Pause M, Kunesch E, Binkofski F, Freund H-J. Sensorimotor disturbances in patients with lesions of the parietal cortex. *Brain* 112: 1599–1625, 1989.

Raos V, Franchi G, Gallese V, Fogassi L. Somatotopic organization of the lateral part of area F2 (dorsal premotor cortex) of the macaque monkey. *J Neurophysiol* 89: 1503–1518, 2003.

Raos V, Umilta MA, Gallese V, Fogassi L. Functional properties of grasping-related neurons in the dorsal premotor area F2 of the macaque monkey. *J Neurophysiol* 92: 1990–2002, 2004.

Raos V, Umilta MA, Murata A, Fogassi L, Gallese V. Functional properties of grasping-related neurons in the ventral premotor area F5 of the macaque monkey. *J Neurophysiol* 95: 709–729, 2006.

Rice NJ, Tunik E, Hamilton A, Grafton ST. The anterior intraparietal sulcus mediates grasp execution, independent of requirement to update: new insights from transcranial magnetic stimulation. *J Neurosci* 26: 8176–8182, 2006.

Rizzolatti G, Luppino G. The cortical motor system. *Neuron* 31: 889–901, 2001.

Ro JY, Debowy D, Ghosh S, Gardner EP. Depression of neuronal activity in somatosensory and posterior parietal cortex during prehension. *Exp Brain Res* 135: 1–11, 2000.

Ro JY, Debowy D, Lu S, Ghosh S, Gardner EP. Digital video: a tool for correlating neuronal firing patterns with hand motor behavior. *J Neurosci Methods* 82: 215–231, 1998.

Roy A, Paulignan Y, Meunier M, Boussaoud D. Prehension movements in the macaque monkey: effects of object size and location. *J Neurophysiol* 88: 1491–1499, 2002.

Sakata H, Taira M, Kusunoki M, Murata A, Tanaka Y. The parietal association cortex in depth perception and visual control of hand action. *Trends Neurosci* 20: 350–357, 1997.

Sakata H, Taira M, Murata A, Mine S. Neural mechanisms of visual guidance of hand action in the parietal cortex of the monkey. *Cereb Cortex* 5: 429–438, 1995.

Santello M, Flanders M, Soechting JF. Postural hand synergies for tool use. *J Neurosci* 18: 10105–10115, 1998.

Santello M, Flanders M, Soechting JF. Patterns of hand motion during grasping and the influence of sensory guidance. *J Neurosci* 22: 1426–1435, 2002.

Seltzer B, Pandya DN. Converging visual and somatic sensory cortical input to the intraparietal sulcus of the rhesus monkey. *Brain Res* 192: 339–351, 1980.

Sherwood A, Lang EJ, Gardner EP. The neuroinformatics digital video toolkit. *Soc Neurosci Abstr* 32: 147.6, 2006.

Shikata E, Hamzei F, Glauche V, Koch M, Weiller C, Binkofski F, Buchel C. Functional properties and interaction of the anterior and posterior intraparietal areas in humans. *Eur J Neurosci* 17: 1105–1110, 2003.

Shmuelof L, Zohary E. Dissociation between ventral and dorsal fMRI activation during object and action recognition. *Neuron* 47: 457–470, 2005.

Srinivasan MA, LaMotte RH. Tactile discrimination of shape: responses of slowly and rapidly adapting mechanoreceptive afferents to a step indented into the monkey fingerpad. *J Neurosci* 7: 1682–1697, 1987.

Stoeckel MC, Weder B, Binkofski F, Choi HJ, Amunts K, Pieperhoff P, Shah NJ, Seitz RJ. Left and right superior parietal lobule in tactile object discrimination. *Eur J Neurosci* 19: 1067–1072, 2004.

Taira M, Mine S, Georgopoulos AP, Murata A, Sakata H. Parietal cortex neurons of the monkey related to the visual guidance of hand movement. *Exp Brain Res* 83: 29–36, 1990.

Theverapperuma LS, Hendrix CM, Mason CR, Ebner TJ. Finger movements during reach-to-grasp in the monkey: amplitude scaling of a temporal synergy. *Exp Brain Res* 169: 433–438, 2006.

Tunik E, Frey S, Grafton S. Virtual lesions of the anterior intraparietal area disrupt goal-dependent on-line adjustments of grasp. *Nat Neurosci* 8: 505–511, 2005.

Tunik E, Rice NJ, Hamilton A, Grafton ST. Beyond grasping: representation of action in human anterior intraparietal sulcus. *NeuroImage* 36: T77–T86, 2007.

Umilta MA, Brochier T, Spinks R, Lemon RN. Simultaneous recording of macaque premotor and primary motor cortex neuronal populations reveals different functional contributions to visuomotor grasp. *J Neurophysiol* 98: 488–501, 2007.

Wenderoth N, Toni I, Bedeleem S, Debaere F, Swinnen SP. Information processing in human parieto-frontal circuits during goal-directed bimanual movements. *Neuroimage* 31: 264–278, 2006.

Westling G, Johansson RS. Factors influencing the force control during precision grip. *Exp Brain Res* 53: 277–284, 1984.

Westling G, Johansson RS. Responses in glabrous skin mechanoreceptors during precision grip in humans. *Exp Brain Res* 66: 128–140, 1987.

Wise SP, Boussaoud D, Johnson PB, Caminiti R. Premotor and parietal cortex: corticocortical connectivity and combinatorial computations. *Annu Rev Neurosci* 20: 25–42, 1997.